AD-A138 370 DETAILED FLOW MEASUREMENTS IN CASING BOUNDARY LAYER OF 429-METER-PER-SECO..(U) NATIONAL AERONAUTICS AND SPACE ADMINISTRATION CLEVELAND OH LE.. W T GORRELL JAN 84 1/1

UNCLASSIFIED NASA-E-219 NASA-TP-2052 F/G 20/4 NL

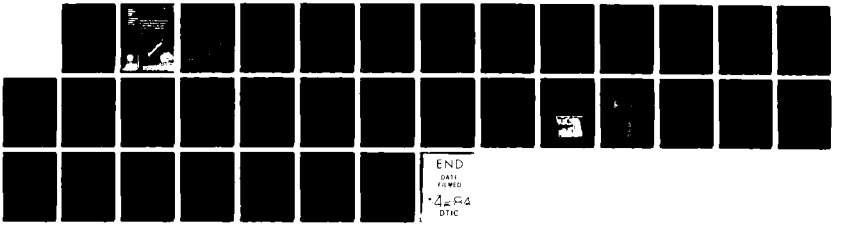

END

DATE FILMED

4-84

DTIC

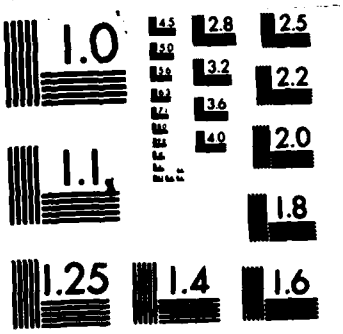

MICROCOPY RESOLUTION TEST CHART
NATIONAL BUREAU OF STANDARDS 1963-A

NASA Technical Paper 2052

AVRADCOM Technical Report 81-C-28

1984

Detailed Flow Measurements in Casing Boundary Layer of 429-Meter-per-Second-Tip-Speed Two-Stage Fan

William T. Gorrell

Propulsion Laboratory
AVRADCOM Research and Technology Laboratories
Lewis Research Center
Cleveland, Ohio

Corrected Copy

National Aeronautics and Space Administration

Scientific and Technical Information Office

1984

Summary

Detailed flow measurements made in the casing boundary layer of a two-stage transonic fan are summarized. These measurements were taken at stations upstream of the fan, between all blade rows, and downstream of the last blade row. At the design tip speed (429 m/sec) the fan achieved a peak efficiency of 0.846 at a pressure ratio of 2.471. The boundary layer data were obtained at three weight flows at the design speed: one near choke flow, one near peak efficiency, and one near stall. The data presented show steep axial velocity profiles at the fan inlet and at both rotor exits. The axial velocity profiles at the stator exits were not as steep as those at the rotor exits. The data also show overturning of the flow at the tip at the stator exits. The effect of mixing is shown by the redistribution of the first-stage rotor-exit total temperature profile as it passes through the following stator.

Introduction

The Lewis Research Center has been investigating the aerodynamic performance of a two-stage fan with a design pressure ratio of 2.40 (refs. 1 to 5). This investigation is part of a program to demonstrate improved performance of highly loaded, multistage, axial-flow compressors. Analysis of the results from references 2 to 5 indicated that the first-stage stator and the second stage had potential for good performance but were hampered mainly by the dampered first-stage rotor. In an effort to improve performance of the first stage, as well as to improve stage matching, the first-stage rotor was redesigned. Lower-aspect-ratio blading was selected for the rotor to eliminate the part-span damper and its adverse effect on performance. An inlet-tip boundary-layer total pressure, based on unreported boundary-layer survey data taken with the configuration of reference 3, and an end-wall blockage allowance, was incorporated into the new design, resulting in the rotor blading having leading-edge end-wall bend. It was anticipated that the leading edge of the rotor blade would be alined to the flow in the casing boundary layer. The performance of the low-aspect-ratio fan is reported in reference 1. Results show that the flow in the tip region of the first-stage rotor was not well alined with the blade and losses remained high.

More detailed information than is currently available about the flow in the end-wall regions, particularly in the multistage environment, is needed to develop improved end-wall designs. The wide blade-row spacing of this two-stage fan afforded the opportunity to measure the flow field in the outer-wall region behind each blade row.

The data resulting from these measurements are presented in this report in both tabular and plotted form. Design-speed data were recorded at three flow conditions. The symbols and equations are defined in appendixes A and B.

Apparatus and Procedure

Two-Stage Fan

The low-aspect-ratio two-stage fan was designed to produce a 2.40:1 pressure ratio at 427-meter-per-second tip speed. The two-stage fan was designed with a computer program described in reference 6. A measured inlet-radial total-pressure distribution in the casing boundary layer (ref. 3) was used to model the total-pressure profile in the inlet end-wall region in the design of the low-aspect-ratio first-stage rotor described in reference 1. The computer program used in the design was unable to handle the steep total-pressure gradient from the measurements. To alleviate this problem, the total-pressure distribution was modified and combined with an end-wall blockage of 0.01. It was hoped that this would aline the blade with the flow entering the rotor at the tip, resulting in reduced losses. At the other stations in the two-stage fan, blockage allowances were the only method used to account for the hub and casing boundary layers. The blockage allowances at the tip were 0.013 at the first-stage rotor exit, 0.017 at the first-stage stator inlet, and 0.020 at all other stations. Blockage allowances at the hub were the same as at the tip at each station. Design diffusion factors at the tip of the first- and second-stage rotors are 0.451 and 0.410, respectively, and at the first- and second-stage stators, 0.472 and 0.464, respectively. The flow path and axial locations of the measuring stations are shown in figure 1. Figure 2 shows the fan with casing treatment over the rotors. However, when taking the boundary layer data, solid inserts were installed over the rotor tips.

Compressor Test Facility

The two-stage fan was tested in the multistage compressor facility (ref. 2). A schematic diagram of the facility is shown in figure 3. Atmospheric air enters the test facility at an inlet located on the roof of the building and flows through the flow measuring orifice, through the inlet butterfly throttle valves, and into the plenum chamber upstream of the test fan. The air then passes through the test fan into the collector and is exhausted either to the atmosphere or to an altitude exhaust system. Mass flow is controlled with a sleeve valve in the collector. For this series of tests the large inlet butterfly

valve remained fully open with the small valve fully closed, and the air was exhausted to the atmosphere.

Instrumentation

Radial surveys of the flow conditions between 1 and 30 percent of passage height were made at the fan inlet, behind each rotor, and behind the two stator-blade rows (see fig. 1). Total pressure, total temperature, and flow angle were measured with combination probes (fig. 4). Static pressure was measured with the combination probes and wall static taps at each measuring station. Each probe was positioned with a null-balancing, stream-direction-sensitive control system. The thermocouple material was Chromel-constantan. All pressures were measured with calibrated transducers. Two combination probes were used at the compressor inlet, behind each rotor, and behind the first-stage stator. Four combination probes were used behind the second-stage stator. The circumferential locations of the probes and wall static taps at each measuring station are shown in figure 5. The probes behind the stators were circumferentially traversed one stator-blade passage clockwise from the nominal values shown. The fan mass flow was determined with a calibrated thin-plate orifice located in the inlet line. An electronic speed counter, in conjunction with a magnetic pickup, was used to measure rotative speed (rpm).

The estimated errors of the data, based on inherent accuracies of the recording system, are as follows:

Mass flow, kg/sec	±0.3
Rotative speed, rpm	±30
Flow angle, deg	±1
Temperature, K	±0.6
Total pressure (stations 1 and 2), N/cm^2	±0.07
Total pressure (station 3), N/cm^2	±0.10
Total pressure (stations 4 and 5), N/cm^2	±0.17
Indicated static pressure (stations 1, 2, and 3), N/cm^2	±0.07
Indicated static pressure (stations 4 and 5), N/cm^2	±0.17
Radial position, cm	±0.003

Test Procedure

The data for the boundary-layer surveys were taken at three mass flows from maximum flow to near stall, at an equivalent rotative speed of 100 percent of design speed. At each selected flow, data were recorded at 10 radial positions at each of the five measuring stations. At the fan-inlet and rotor-exit stations (stations 1, 2, and 4) radial traverses were made to measure total pressure, static pressure, total temperature, and flow angle at each radial position. At each radial position the combination probes behind the stators (stations 3 and 5) were circumferentially traversed to 10 equally spaced locations across a stator-blade gap. Total pressure, static pressure, total temperature, and flow angle were measured at each circumferential position.

Data Reduction

Redundant measurements at each measuring station (two at stations 1, 2, 3, and 4) were arithmetically averaged. Indicated total pressures, static pressures, and total temperatures were corrected for Mach number and streamline slope (ref. 7). All data were corrected to standard-day conditions based on values at 30 percent of the passage height at the first-stage rotor inlet. To get representative radial distributions in addition to the circumferential distributions at the stator exits, the circumferential distributions of total temperature were mass averaged; total pressure was energy averaged; and flow angle was arithmetically averaged at each radial position. The Mach number at each radial position behind a rotor and at each radial and circumferential position behind a stator is calculated from the measured total pressure at each radial and circumferential position and the static pressure at each radial position. Absolute velocity was calculated from the Mach number and measured total temperature. Absolute velocity and measured flow angle were used to calculate axial and tangential velocity components.

Determination of Static Pressure

Total pressure, total temperature, and flow angle measurements were taken at 10 radial positions between 1 and 30 percent of passage height from the casing. Because measurements were not taken across the full passage height, static pressure could not be calculated as was done in reference 1. To acquire static pressures for the boundary-layer surveys, the side balancing holes on the combination probes (fig. 4) were manifolded to read an indicated static pressure. Figure 6 is a comparison of the measured static pressures at station 1 from the boundary-layer surveys at a mass flow of 34.23 kg/sec and calculated static pressures from earlier, unreported full-passage-height surveys, also at 34.23 kg/sec. At 30 percent of passage height, the measured static pressure is significantly lower than the calculated static pressure.

The static pressures were calculated using design end-wall blockage values. It would appear that, if the blockage value were adjusted until the calculated value at 5 percent of passage height matched the wall static value, the calculated value at 30 percent of passage height would nearly equal the measured value as well.

Since the accuracy of the static-pressure measurement is uncertain near the casing, it was arbitrarily decided that a linear distribution of static pressure between the wall static and the measurement at 30 percent of passage height would be used to reduce the boundary-layer survey

data. However, all measured static pressures are presented in table I.

Results and Discussion

The overall and stage performance of the two-stage fan are presented in figures 7 and 8. Figures 9 to 13 are radial distributions of various flow parameters between 1 and 30 percent of passage height at each measuring station. Figure 14 presents radial and circumferential distributions of axial velocity at the stator exits. The data in these figures are presented in tables II to VIII.

Overall and Stage Performance

The overall performance of the two-stage fan with the low-aspect-ratio first-stage rotor is presented in figure 7. At the design tip speed of 429 m/sec the fan achieved a peak efficiency of 0.846 at a pressure ratio of 2.471. Arrows pointing to the design speed line indicate the locations where the boundary layer data were obtained. The stage performance is given in figure 8. The first stage achieved a peak efficiency of 0.870 at a pressure coefficient of 0.257 (pressure ratio = 1.655). The second stage achieved a peak efficiency of 0.842 at a pressure coefficient of 0.260 (pressure ratio = 1.494).

Radial Distributions at Measuring Stations

The results presented in figures 9 to 13 are presented at three mass flows at design speed, 34.63 kg/sec (choke), 34.23 kg/sec (peak efficiency), and 34.01 kg/sec (near stall). The solid lines in the figures are design values, and the symbols are measured values.

First-stage rotor inlet (station 1). – The axial velocity is higher than design over most of the outer 30 percent of the passage height (fig. 9). This velocity difference is due, in part, to the mass flow being higher than design and in part to the selection of static pressure. However, the measured velocity decreases much more rapidly from 4 to 1 percent of the passage height than the design values. The total-pressure gradient along with the 0.010 outer wall blockage used in the design at the rotor inlet did not accurately model the casing boundary layer.

First- and second-stage rotor exits (stations 2 and 4). – The axial velocity distributions at the exits of the first- and second-stage rotors are very similar (figs. 10 and 12). The absolute flow angle is much higher than design in the outer 10 percent of passage height which increases incidence angles on the following stators.

First- and second-stage stator exits (stations 3 and 5). – The decrease in axial velocity from 10 to 1 percent of passage height at the stator-exit measuring stations (figs. 11 and 13) is much less than at the rotor-exit measuring stations (figs. 10 and 12). A comparison of figures 10 and 11 shows that the total-temperature profile that left the first-stage rotor was redistributed as it passed through the following stator. Measured total temperatures between 1 and 8 percent of passage height at the stator exit are lower than the corresponding values at the rotor exit. Conversely, total temperatures between 8 and 30 percent of passage height are higher at the first-stage stator exit than at the first-stage rotor exit. This redistribution of total temperature is a result of mixing. The plots of absolute flow angle show overturning of the flow near the casing of 6° at the first-stage stator exit and 4° at the second-stage stator exit.

Circumferential Distributions at Stator Exit Stations

The radial and circumferential distributions of axial velocity behind the first- and second-stage stators (stations 3 and 5) are plotted in figure 14. The data plotted in this figure are at a mass flow of 34.23 kg/sec. For clarity, only 5 of the 10 radial positions at each station are plotted. The wakes behind both stators are less pronounced at 30 percent of the passage height than at 3 or 4 percent of the passage height. The wake also appears to shift circumferentially toward the pressure side of the blade near the tip of both stators. The axial velocity at the edge of the wake on the suction side of the blade is significantly lower than the corresponding velocity on the pressure side at the tip. This velocity imbalance exists at 1 and 2 percent of passage height and is nearly gone at 3 or 4 percent of passage height.

Concluding Remarks

Secondary flows in compressor blade rows arise from the inability of the end-wall boundary layers to sustain the blade-to-blade static-pressure gradient. Several aspects of the data discussed earlier suggest the presence of strong secondary flows in both stator-blade rows. The velocity imbalance across the stator wakes is the result of an accumulation of low-energy boundary-layer fluid near the suction surface caused by secondary flows. The redistribution of total temperature is also a result of secondary flows as well as of turbulence. It is this mixing that accounts for the stator-exit axial velocity profiles being much flatter than the rotor-exit profiles.

This suggests that casing blockage effects in multistage compressors are reduced by mixing. The high stator incidence angles that will result from the highly skewed flow in the casing boundary layer exiting the rotors reinforces the secondary flows generated in the stators. This reinforcement is a result of the low pressure (lower

than at lower incidence angles) that occurs on the suction surface as a result of the high incidence angles. The overturning, as well, is the result of secondary flows.

Summary of Results

This report presents detailed measurements of the casing boundary layer in a 429-meter-per-second-tip-speed, two-stage fan. The fan achieved a peak adiabatic efficiency of 0.846 at a pressure ratio of 2.471 at design speed. The following principal results were obtained:

1. Axial velocities at the first-stage rotor inlet and at both rotor exits decreased more rapidly from 4 percent of the passage height to the casing than the design values.

2. The absolute flow angle distribution at the exit of both stators shows approximately 4° of overturning near the tip. This overturning is most likely the result of secondary flows.

3. The decrease in axial velocity from 10 percent to 1 percent of passage height at the stator-exit measuring stations is much less than at the rotor exit measuring stations.

Lewis Research Center
National Aeronautics and Space Administration,
Cleveland, Ohio, May 7, 1982

Appendix A
Symbols

C_p specific heat at constant pressure, 1004 J/kg·K
D diffusion factor
N rotative speed, rpm
P total pressure, N/cm^2
p static pressure, N/cm^2
r radius, cm
T total temperature, K
U wheel speed, m/sec
V air velocity, m/sec
W weight flow, kg/sec
Z axial distance referenced from rotor-blade-hub leading edge, cm
β' relative air angle (angle between air velocity and axial direction), deg
γ ratio of specific heats
δ ratio of rotor-inlet total pressure to standard pressure of 10.13 N/cm^2
η efficiency
θ ratio of rotor-inlet total temperature to standard temperature of 288.2 K
σ solidity; ratio of chord to spacing

Subscripts:

ad adiabatic (temperature rise)
LE blade leading edge
p polytropic
TE blade trailing edge
t tip
z axial direction
θ tangential direction
1 instrumentation plane upstream of first rotor
2 instrumentation plane downstream of first rotor
3 instrumentation plane downstream of first stator
4 instrumentation plane downstream of second rotor
5 instrumentation plane downstream of second stator

Superscript:

' relative to blade

Appendix B
Equations

Diffusion factor—

$$D = 1 - \frac{V'_{TE}}{V'_{LE}} + \frac{(rV_\theta)_{TE} - (rV_\theta)_{LE}}{(r_{TE} + r_{LE})\sigma(V'_{LE})} \quad \text{(B1)}$$

Percent of passage height—

$$\frac{(r_t - r)}{(r_t - r_h)} 100 \quad \text{(B2)}$$

Adiabatic (temperature rise) efficiency—

$$\eta_{ad} = \frac{\left(\frac{P_{TE}}{P_{LE}}\right)^{(\gamma-1)/\gamma} - 1}{\frac{T_{TE}}{T_{LE}} - 1} \quad \text{(B3)}$$

Equivalent mass flow—

$$W\sqrt{\theta/\delta} \quad \text{(B4)}$$

Equivalent rotative speed—

$$\frac{N}{\sqrt{\theta}} \quad \text{(B5)}$$

Head-rise coefficient—

$$\psi_P = \frac{C_p T_{LE}}{U_{tip}^2}\left(\frac{P_{TE}}{P_{LE}}\right)^{(\gamma-1)/\gamma} - 1 \quad \text{(B6)}$$

Flow coefficient—

$$\varphi = \frac{V_z}{U_{tip}} \text{LE} \quad \text{(B7)}$$

Polytropic efficiency—

$$\eta_p = \frac{\ln\left(\frac{P_{TE}}{P_{LE}}\right)^{(\gamma-1)/\gamma}}{\ln \frac{T_{TE}}{T_{LE}}} \quad \text{(B8)}$$

Temperature-rise coefficient—

$$\psi_T = \frac{C_p(T_{TE} - T_{LE})}{U_{tip}^2} \quad \text{(B9)}$$

Relative flow angle—

$$\beta' = \arctan\left(\frac{V'_\theta}{V_z}\right) \quad \text{(B10)}$$

References

1. Urasek, Donald C.; Gorrell, William T.; and Cunnan, Walter S.: Performance of a Two-Stage Fan Having Low-Aspect-Ratio First-Stage Rotor Blading. NASA TP-1493; AVRADCOM TR 78-49, 1979.
2. Cunnan, Walter S.; Stevans, William; and Urasek, Donald C.: Design and Performance of a 427-Meters-per-Second-Tip-Speed Two-Stage Fan Having a 2.40 Pressure Ratio. NASA TP-1314, 1978.
3. Urasek, Donald C.; Cunnan, Walter S.; and Stevans, William: Performance of Two-Stage Fan with Larger Dampers on First-Stage Rotor. NASA TP-1399, 1979.
4. Gorrell, William T.; and Urasek, Donald C.: Performance of Two-Stage Fan with a First-Stage Rotor Redesigned to Account for the presence of a Part-Span Damper. NASA TP-1483, AVRADCOM TR 79-10, 1979.
5. Urasek, Donald C.: Effect of Casing Treatment on Performance of a Two-Stage High-Pressure Ratio Fan. NASA TP-1409, 1979.
6. Ball, Calvin L.; Janetzke, David C.; and Reid, Lonnie: Performance of 1380-Foot-Per-Second-Tip-Speed Axial Flow Compressor Rotor with Blade Tip Solidity of 1.1. NASA TM X-2449, 1972.
7. Glawe, George E.; Krause, Lloyd N.; and Dudzinski, Thomas J.: A Small Combination Sensing Probe for Measurement of Temperature, Pressure, and Flow Direction. NASA TN D-4816, 1968.

TABLE I. – MEASURED STATIC PRESSURES

(a) First-Stage Rotor Inlet.

MASS FLOW KG/SEC	34.63	34.23	34.01	
PERCENT PASSAGE HEIGHT				
0.00	8.15	8.21	8.22	(WALL STATIC)
1.00	8.42	8.45	8.48	
2.00	8.41	8.43	8.47	
3.00	8.41	8.43	8.48	
4.00	8.42	8.43	8.49	
6.00	8.40	8.41	8.46	
8.00	8.34	8.37	8.42	
10.00	8.30	8.31	8.36	
15.00	8.13	8.16	8.20	
20.00	8.00	8.01	8.06	
30.00	7.82	7.82	7.86	

(b) First-Stage Rotor Inlet.

MASS FLOW KG/SEC	34.63	34.23	34.01	
PERCENT PASSAGE HEIGHT				
0.00	12.40	13.08	13.21	(WALL STATIC)
1.00	12.62	13.33	13.47	
2.00	12.54	13.24	13.40	
3.00	12.52	13.22	13.38	
4.00	12.50	13.20	13.36	
6.00	12.44	13.12	13.29	
8.00	12.43	13.09	13.24	
10.00	12.40	13.02	13.16	
15.00	12.21	12.77	12.85	
20.00	11.92	12.44	12.55	
30.00	11.55	12.12	12.26	

(c) First-Stage Stator Exit.

MASS FLOW KG/SEC	34.63	34.23	34.01	
PERCENT PASSAGE HEIGHT				
0.00	13.47	14.27	14.41	(WALL STATIC)
1.00	13.65	14.45	14.62	
2.00	13.62	14.41	14.58	
3.00	13.59	14.39	14.56	
4.00	13.59	14.38	14.55	
6.00	13.57	14.36	14.52	
8.00	13.54	14.31	14.48	
10.00	13.51	14.28	14.45	
15.00	13.43	14.18	14.3	
20.00	13.33	4.07	42	
30.00	13.09	13.8	13.97	

(d) Second-Stage Rotor Exit.

MASS FLOW KG/SEC	34.63	34.23	34.01	
PERCENT PASSAGE HEIGHT				
0.00	19.04	20.77	20.92	(WALL STATIC)
1.00	19.31	21.04	21.20	
2.00	19.22	20.85	20.99	
3.00	19.15	20.71	20.89	
4.00	19.11	20.68	20.84	
6.00	19.10	20.67	20.80	
8.00	19.08	20.60	20.76	
10.00	19.04	20.62	20.81	
15.00	18.95	20.51	20.64	
20.00	18.67	20.15	20.28	
30.00	18.22	19.74	19.90	

(e) Second-Stage Stator Exit.

MASS FLOW KG/SEC	34.63	34.23	34.01	
PERCENT PASSAGE HEIGHT				
0.00	20.09	22.10	22.25	(WALL STATIC)
1.00	20.22	22.23	22.39	
2.00	20.18	22.18	22.35	
3.00	20.17	22.15	22.29	
4.00	20.15	22.13	22.28	
6.00	20.16	22.16	22.29	
8.00	20.18	22.14	22.28	
10.00	20.17	22.13	22.26	
15.00	20.15	22.07	22.23	
20.00	20.08	22.04	22.18	
30.00	19.86	21.84	21.95	

TABLE II. – RADIAL DISTRIBUTIONS FOR FIRST-STAGE ROTOR INLET

MASS FLOW = 34.63 KG/SEC

PERCENT PASSAGE HEIGHT	RADIUS CM	AXIAL VEL. M/SEC	TANG. VEL. M/SEC	TOTAL TEMP. DEG. K	TOTAL PRESS. N/CM**2	ABS. FLOW ANG. DEG.	REL. FLOW ANG. DEG.	STATIC PRESS. N/CM**2
1.0	25.49	146.75	0.00	289.38	9.29	0.00	71.09	8.14
2.0	25.33	160.42	0.00	289.32	9.53	0.00	69.34	8.13
3.0	25.17	169.80	0.00	289.36	9.70	0.00	68.12	8.12
4.0	25.01	177.08	0.00	289.21	9.85	0.00	67.15	8.11
6.0	24.69	185.57	0.00	289.33	10.01	0.00	65.89	8.09
8.0	24.36	189.41	0.00	288.93	10.08	0.00	65.17	8.06
10.0	24.04	191.41	0.00	288.78	10.10	0.00	64.64	8.04
15.0	23.24	195.01	0.00	288.51	10.13	0.00	63.45	7.99
20.0	22.43	197.98	0.00	288.28	10.13	0.00	62.28	7.93
30.0	20.82	203.36	0.00	288.17	10.13	0.00	59.82	7.82

MASS FLOW = 34.23 KG/SEC

PERCENT PASSAGE HEIGHT	RADIUS CM	AXIAL VEL. M/SEC	TANG. VEL. M/SEC	TOTAL TEMP. DEG. K	TOTAL PRESS. N/CM**2	ABS. FLOW ANG. DEG.	REL. FLOW ANG. DEG.	STATIC PRESS. N/CM**2
1.0	25.49	143.56	0.00	291.01	9.30	0.00	71.47	8.20
2.0	25.33	157.13	0.00	290.38	9.53	0.00	69.73	8.19
3.0	25.17	166.76	0.00	290.14	9.70	0.00	68.48	8.18
4.0	25.01	173.98	0.00	290.13	9.84	0.00	67.51	8.16
6.0	24.69	182.65	0.00	289.67	10.01	0.00	66.23	8.14
8.0	24.36	186.77	0.00	289.35	10.07	0.00	65.47	8.11
10.0	24.04	189.33	0.00	289.30	10.10	0.00	64.88	8.09
15.0	23.24	193.77	0.00	289.23	10.13	0.00	63.60	8.02
20.0	22.43	196.80	0.00	288.72	10.13	0.00	62.42	7.96
30.0	20.82	202.91	0.00	288.17	10.13	0.00	59.88	7.83

MASS FLOW = 34.01 KG/SEC

PERCENT PASSAGE HEIGHT	RADIUS CM	AXIAL VEL. M/SEC	TANG. VEL. M/SEC	TOTAL TEMP. DEG. K	TOTAL PRESS. N/CM**2	ABS. FLOW ANG. DEG.	REL. FLOW ANG. DEG.	STATIC PRESS. N/CM**2
1.0	25.49	143.45	0.00	289.49	9.31	0.00	71.48	8.21
2.0	25.33	156.18	0.00	289.31	9.52	0.00	69.85	8.19
3.0	25.17	166.58	0.00	289.31	9.71	0.00	68.50	8.18
4.0	25.01	174.50	0.00	289.62	9.86	0.00	67.44	8.17
6.0	24.69	182.10	0.00	289.41	10.01	0.00	66.29	8.15
8.0	24.36	186.78	0.00	289.17	10.09	0.00	65.47	8.12
10.0	24.04	188.25	0.00	289.01	10.10	0.00	65.01	8.10
15.0	23.24	192.69	0.00	288.72	10.13	0.00	63.73	8.04
20.0	22.43	195.61	0.00	288.61	10.13	0.00	62.56	7.98
30.0	20.82	201.28	0.00	288.17	10.13	0.00	60.08	7.86

TABLE III. – RADIAL DISTRIBUTIONS FOR FIRST-STAGE ROTOR EXIT

MASS FLOW = 34.63 KG/SEC

PERCENT PASSAGE HEIGHT	RADIUS CM	AXIAL VEL. M/SEC	TANG. VEL. M/SEC	TOTAL TEMP. DEG. K	TOTAL PRESS. N/CM**2	ABS. FLOW ANG. DEG.	REL. FLOW ANG. DEG.	STATIC PRESS. N/CM**2
1.0	24.34	114.78	153.76	351.73	14.92	53.26	65.77	12.38
2.0	24.21	124.85	155.67	350.55	15.14	51.27	63.56	12.35
3.0	24.08	136.22	153.75	350.14	15.30	48.46	61.50	12.32
4.0	23.96	148.25	151.07	349.65	15.48	45.54	59.47	12.29
6.0	23.71	173.17	142.09	345.85	15.90	39.37	55.94	12.23
8.0	23.45	190.59	134.55	342.15	16.25	35.22	53.70	12.18
10.0	23.21	199.44	130.16	338.78	16.43	33.13	52.47	12.12
15.0	22.58	206.35	129.44	335.72	16.53	32.10	50.44	11.98
20.0	21.95	209.09	133.15	334.12	16.56	32.49	48.41	11.84
30.0	20.69	209.17	142.58	332.96	16.43	34.28	44.43	11.55

MASS FLOW = 34.23 KG/SEC

PERCENT PASSAGE HEIGHT	RADIUS CM	AXIAL VEL. M/SEC	TANG. VEL. M/SEC	TOTAL TEMP. DEG. K	TOTAL PRESS. N/CM**2	ABS. FLOW ANG. DEG.	REL. FLOW ANG. DEG.	STATIC PRESS. N/CM**2
1.0	24.34	122.67	164.58	357.85	16.13	53.30	63.33	13.06
2.0	24.21	131.80	165.35	356.61	16.32	51.44	61.36	13.03
3.0	24.08	142.11	163.25	356.44	16.47	48.96	59.51	13.00
4.0	23.96	152.94	160.04	354.71	16.64	46.30	57.75	12.96
6.0	23.71	174.01	153.36	351.54	17.02	41.39	54.60	12.90
8.0	23.45	186.03	147.82	347.49	17.24	38.47	52.92	12.84
10.0	23.21	192.01	143.48	344.58	17.29	36.77	52.07	12.77
15.0	22.58	198.04	140.95	340.79	17.29	35.44	50.27	12.61
20.0	21.95	199.31	144.96	339.42	17.26	36.03	48.31	12.45
30.0	20.69	201.47	154.42	337.84	17.20	37.47	43.80	12.13

MASS FLOW = 34.01 KG/SEC

PERCENT PASSAGE HEIGHT	RADIUS CM	AXIAL VEL. M/SEC	TANG. VEL. M/SEC	TOTAL TEMP. DEG. K	TOTAL PRESS. N/CM**2	ABS. FLOW ANG. DEG.	REL. FLOW ANG. DEG.	STATIC PRESS. N/CM**2
1.0	24.34	127.74	164.92	359.11	16.38	52.24	62.36	13.18
2.0	24.21	135.58	164.82	356.76	16.54	50.56	60.73	13.15
3.0	24.08	146.15	162.26	355.64	16.70	47.99	58.91	13.11
4.0	23.96	156.85	160.51	354.98	16.91	45.66	57.05	13.08
6.0	23.71	175.20	156.54	351.24	17.31	41.78	54.06	13.02
8.0	23.45	185.16	151.66	348.10	17.47	39.32	52.62	12.96
10.0	23.21	190.00	147.22	345.69	17.47	37.77	51.93	12.89
15.0	22.58	194.68	144.53	341.79	17.42	36.59	50.33	12.74
20.0	21.95	194.93	148.34	339.99	17.35	37.27	48.51	12.58
30.0	20.69	198.23	156.04	337.85	17.31	38.21	44.02	12.26

TABLE IV. – RADIAL DISTRIBUTIONS FOR FIRST-STAGE STATOR EXIT

MASS FLOW = 34.63 KG/SEC

PERCENT PASSAGE HEIGHT	RADIUS CM	AXIAL VEL. M/SEC	TANG. VEL. M/SEC	TOTAL TEMP. DEG. K	TOTAL PRESS. N/CM**2	ABS. FLOW ANG. DEG.	REL. FLOW ANG. DEG.	STATIC PRESS. N/CM**2
1.0	24.27	143.01	-13.83	345.29	14.95	-5.52	71.26	13.45
2.0	24.16	150.99	-11.00	345.04	15.12	-4.17	70.09	13.44
3.0	24.04	157.89	-6.51	345.24	15.27	-2.36	68.96	13.43
4.0	23.93	163.05	-5.24	344.43	15.39	-1.84	68.18	13.42
6.0	23.70	170.69	-0.55	343.99	15.57	-0.18	66.83	13.39
8.0	23.47	176.01	-1.51	342.60	15.70	-0.49	66.03	13.36
10.0	23.25	180.44	-0.52	340.77	15.82	-0.17	65.23	13.34
15.0	22.68	191.71	-3.11	337.83	16.13	-0.93	63.48	13.28
20.0	22.11	196.47	-1.87	336.34	16.23	-0.55	62.25	13.21
30.0	20.98	199.90	-5.14	334.81	16.22	-1.47	60.79	13.09

MASS FLOW = 34.23 KG/SEC

PERCENT PASSAGE HEIGHT	RADIUS CM	AXIAL VEL. M/SEC	TANG. VEL. M/SEC	TOTAL TEMP. DEG. K	TOTAL PRESS. N/CM**2	ABS. FLOW ANG. DEG.	REL. FLOW ANG. DEG.	STATIC PRESS. N/CM**2
1.0	24.27	147.74	-14.86	354.42	15.92	-5.75	70.73	14.26
2.0	24.16	156.38	-11.98	353.02	16.12	-4.38	69.48	14.24
3.0	24.04	163.00	-5.71	352.37	16.27	-2.00	68.30	14.23
4.0	23.93	167.89	-5.43	351.71	16.39	-1.85	67.60	14.21
6.0	23.70	174.44	1.16	350.31	16.55	0.38	66.28	14.18
8.0	23.47	178.06	-0.51	348.51	16.64	-0.16	65.73	14.15
10.0	23.25	181.09	1.01	347.07	16.71	0.32	65.07	14.12
15.0	22.68	188.53	-2.10	344.03	16.90	-0.64	63.80	14.05
20.0	22.11	193.19	-1.54	341.61	16.99	-0.46	62.62	13.97
30.0	20.98	196.95	-4.40	339.13	16.97	-1.28	61.10	13.82

MASS FLOW = 34.01 KG/SEC

PERCENT PASSAGE HEIGHT	RADIUS CM	AXIAL VEL. M/SEC	TANG. VEL. M/SEC	TOTAL TEMP. DEG. K	TOTAL PRESS. N/CM**2	ABS. FLOW ANG. DEG.	REL. FLOW ANG. DEG.	STATIC PRESS. N/CM**2
1.0	24.27	149.95	-14.89	353.67	16.13	-5.67	70.46	14.40
2.0	24.16	158.23	-11.85	352.81	16.32	-4.28	69.25	14.38
3.0	24.04	165.08	-5.35	352.33	16.49	-1.86	68.03	14.37
4.0	23.93	170.39	-4.74	352.48	16.62	-1.59	67.27	14.35
6.0	23.70	176.72	2.27	350.95	16.79	0.74	65.95	14.32
8.0	23.47	180.03	0.92	349.33	16.87	0.29	65.41	14.29
10.0	23.25	182.53	2.42	347.68	16.93	0.76	64.81	14.26
15.0	22.68	188.15	-0.93	344.69	17.05	-0.28	63.78	14.19
20.0	22.11	192.07	-0.43	342.78	17.12	-0.13	62.69	14.12
30.0	20.98	195.57	-3.45	340.11	17.09	-1.01	61.21	13.97

TABLE V. – RADIAL DISTRIBUTIONS FOR SECOND-STAGE ROTOR EXIT

MASS FLOW = 34.63 KG/SEC

PERCENT PASSAGE HEIGHT	RADIUS CM	AXIAL VEL. M/SEC	TANG. VEL. M/SEC	TOTAL TEMP. DEG. K	TOTAL PRESS. N/CM**2	ABS. FLOW ANG. DEG.	REL. FLOW ANG. DEG.	STATIC PRESS. N/CM**2
1.0	23.53	111.79	124.64	395.30	21.56	48.11	67.56	19.01
2.0	23.44	119.01	129.83	397.20	21.81	47.49	65.74	18.98
3.0	23.36	127.54	134.21	398.91	22.09	46.46	63.71	18.96
4.0	23.26	135.64	137.55	400.04	22.36	45.40	61.83	18.93
6.0	23.09	153.32	141.83	399.15	22.96	42.77	58.07	18.87
8.0	22.91	169.74	143.04	399.83	23.49	40.12	54.93	18.82
10.0	22.73	180.94	144.39	398.11	23.92	38.59	52.69	18.77
15.0	22.28	190.10	136.25	392.04	23.96	35.63	51.40	18.63
20.0	21.84	193.98	132.82	387.10	23.93	34.40	50.34	18.49
30.0	20.94	195.59	138.03	383.26	23.88	35.21	47.55	18.22

MASS FLOW = 34.23 KG/SEC

PERCENT PASSAGE HEIGHT	RADIUS CM	AXIAL VEL. M/SEC	TANG. VEL. M/SEC	TOTAL TEMP. DEG. K	TOTAL PRESS. N/CM**2	ABS. FLOW ANG. DEG.	REL. FLOW ANG. DEG.	STATIC PRESS. N/CM**2
1.0	23.53	111.30	162.79	410.65	24.57	55.64	64.42	20.75
2.0	23.44	119.19	162.08	411.11	24.70	53.67	62.78	20.72
3.0	23.36	127.20	163.10	411.88	24.90	52.05	60.98	20.68
4.0	23.26	135.14	164.17	410.89	25.15	50.54	59.19	20.65
6.0	23.09	153.64	164.70	412.47	25.67	46.99	55.45	20.58
8.0	22.91	170.41	162.73	411.71	26.15	43.68	52.50	20.51
10.0	22.73	180.23	160.70	410.48	26.42	41.72	50.82	20.44
15.0	22.28	183.68	150.61	403.21	26.09	39.35	50.62	20.27
20.0	21.84	186.28	146.75	397.83	25.94	38.23	49.75	20.10
30.0	20.94	191.20	152.47	392.78	26.03	38.57	46.20	19.75

MASS FLOW = 34.01 KG/SEC

PERCENT PASSAGE HEIGHT	RADIUS CM	AXIAL VEL. M/SEC	TANG. VEL. M/SEC	TOTAL TEMP. DEG. K	TOTAL PRESS. N/CM**2	ABS. FLOW ANG. DEG.	REL. FLOW ANG. DEG.	STATIC PRESS. N/CM**2
1.0	23.53	111.32	160.23	411.53	24.63	55.21	64.66	20.89
2.0	23.44	122.07	163.11	411.37	24.97	53.19	62.12	20.85
3.0	23.36	127.67	162.76	410.42	25.09	51.89	60.92	20.82
4.0	23.26	137.00	163.85	412.06	25.34	50.10	58.88	20.78
6.0	23.09	155.24	163.93	412.18	25.87	46.56	55.26	20.72
8.0	22.91	169.95	163.32	412.15	26.33	43.86	52.50	20.65
10.0	22.73	178.57	160.84	410.48	26.53	42.01	51.06	20.58
15.0	22.28	182.92	149.93	403.75	26.21	39.34	50.82	20.41
20.0	21.84	184.66	147.04	398.22	26.06	38.53	49.96	20.24
30.0	20.94	189.28	153.17	393.50	26.14	38.98	46.39	19.90

TABLE VI. – RADIAL DISTRIBUTIONS FOR SECOND-STAGE STATOR EXIT

MASS FLOW = 34.63 KG/SEC

PERCENT PASSAGE HEIGHT	RADIUS CM	AXIAL VEL. M/SEC	TANG. VEL. M/SEC	TOTAL TEMP. DEG. K	TOTAL PRESS. N/CM**2	ABS. FLOW ANG. DEG.	REL. FLOW ANG. DEG.	STATIC PRESS. N/CM**2
1.0	23.54	145.82	-12.09	394.24	22.10	-4.74	70.31	20.08
2.0	23.45	152.93	-8.25	394.33	22.30	-3.09	69.18	20.07
3.0	23.37	158.76	-4.55	395.84	22.46	-1.64	68.21	20.06
4.0	23.29	161.90	-2.40	392.66	22.57	-0.85	67.64	20.05
6.0	23.12	167.86	1.77	393.65	22.75	0.60	66.53	20.04
8.0	22.95	172.68	3.65	392.94	22.91	1.21	65.67	20.02
10.0	22.78	176.06	5.38	391.99	23.03	1.75	64.99	20.01
15.0	22.36	182.51	6.27	389.39	23.26	1.97	63.71	19.97
20.0	21.95	186.03	5.16	386.60	23.38	1.59	62.90	19.93
30.0	21.11	190.32	1.65	382.52	23.51	0.50	61.66	19.86

MASS FLOW = 34.23 KG/SEC

PERCENT PASSAGE HEIGHT	RADIUS CM	AXIAL VEL. M/SEC	TANG. VEL. M/SEC	TOTAL TEMP. DEG. K	TOTAL PRESS. N/CM**2	ABS. FLOW ANG. DEG.	REL. FLOW ANG. DEG.	STATIC PRESS. N/CM**2
1.0	23.54	149.36	-9.91	407.31	24.34	-3.79	69.77	22.09
2.0	23.45	155.18	-5.17	406.24	24.52	-1.91	68.76	22.08
3.0	23.37	158.96	-0.74	405.41	24.64	-0.26	67.99	22.07
4.0	23.29	162.61	2.28	405.38	24.76	0.80	67.31	22.06
6.0	23.12	167.73	7.90	404.69	24.94	2.70	66.21	22.04
8.0	22.95	170.69	9.09	403.96	25.04	3.05	65.61	22.03
10.0	22.78	173.15	10.82	403.17	25.13	3.58	65.04	22.01
15.0	22.36	177.54	10.12	400.68	25.27	3.26	64.10	21.97
20.0	21.95	180.91	7.88	397.29	25.39	2.49	63.37	21.92
30.0	21.11	183.40	5.12	390.35	25.46	1.60	62.31	21.84

MASS FLOW = 34.01 KG/SEC

PERCENT PASSAGE HEIGHT	RADIUS CM	AXIAL VEL. M/SEC	TANG. VEL. M/SEC	TOTAL TEMP. DEG. K	TOTAL PRESS. N/CM**2	ABS. FLOW ANG. DEG.	REL. FLOW ANG. DEG.	STATIC PRESS. N/CM**2
1.0	23.54	150.62	-10.50	405.64	24.56	-3.99	69.64	22.24
2.0	23.45	156.27	-5.80	405.28	24.74	-2.13	68.65	22.23
3.0	23.37	158.97	-1.18	404.83	24.82	-0.43	68.02	22.22
4.0	25.32	162.92	1.71	404.46	24.95	0.60	68.96	22.21
6.0	23.12	167.61	7.20	404.05	25.11	2.46	66.26	22.19
8.0	22.95	171.01	8.73	404.11	25.22	2.92	65.59	22.17
10.0	22.78	173.06	10.40	403.31	25.29	3.44	65.07	22.15
15.0	22.36	178.29	10.06	400.69	25.46	3.23	64.01	22.10
20.0	21.95	181.06	7.57	397.59	25.54	2.39	63.37	22.05
30.0	21.11	183.17	5.01	391.62	25.57	1.57	62.35	21.95

TABLE VII. – CIRCUMFERENTIAL DISTRIBUTIONS AT FIRST-STAGE STATOR EXIT

(a) Mass flow, 34.63 kg/sec

RADIUS CM	PERCENT PASSAGE HEIGHT	PERCENT GAP 0.	10.	20.	30.	40.	50.	60.	70.	80.	90.
		TOTAL PRESSURE - N/CM**2									
24.27	1.	15.15	15.25	15.29	14.68	14.51	14.82	14.82	14.81	14.90	15.07
24.16	2.	15.29	15.35	15.39	14.75	14.64	15.09	15.12	15.05	15.09	15.22
24.04	3.	15.40	15.43	15.51	15.05	14.57	15.18	15.36	15.28	15.27	15.37
23.93	4.	15.52	15.54	15.57	15.08	14.62	15.31	15.57	15.46	15.45	15.50
23.70	6.	15.70	15.69	15.70	15.40	14.70	15.15	15.82	15.77	15.71	15.71
23.47	8.	15.83	15.82	15.78	15.39	14.81	15.38	15.97	15.95	15.89	15.87
23.25	10.	15.96	15.93	15.90	15.59	14.93	15.33	16.05	16.12	16.04	16.02
22.68	15.	16.26	16.24	16.20	15.77	15.36	15.90	16.33	16.37	16.34	16.33
22.11	20.	16.36	16.34	16.33	15.98	15.64	15.98	16.36	16.38	16.40	16.40
20.98	30.	16.41	16.41	16.40	15.88	15.80	16.05	16.27	16.25	16.29	16.27
		TOTAL TEMPERATURE - DEG. K									
24.27	1.	344.87	346.69	346.73	346.34	341.67	343.36	343.72	343.76	346.50	348.24
24.16	2.	345.13	345.75	346.49	345.81	342.82	343.57	343.96	344.44	345.61	346.33
24.04	3.	345.73	345.36	346.88	345.66	343.88	344.00	344.63	345.53	345.34	345.01
23.93	4.	345.05	344.25	345.44	345.78	343.10	343.31	343.55	344.27	344.30	345.00
23.70	6.	343.82	344.76	344.97	345.55	342.63	341.93	342.97	343.96	344.50	344.34
23.47	8.	342.82	343.01	343.66	344.30	342.16	340.98	341.32	342.25	342.63	342.81
23.25	10.	337.08	341.36	342.23	342.96	340.76	339.76	340.58	341.04	340.85	341.16
22.68	15.	332.85	338.90	339.24	339.42	337.87	337.55	337.46	338.21	338.20	338.77
22.11	20.	336.11	336.82	336.97	336.90	336.45	335.76	335.68	335.91	336.28	336.51
20.98	30.	335.15	335.56	335.84	335.14	335.01	334.54	334.15	334.20	333.98	334.47
		ABSOLUTE FLOW ANGLE - DEG.									
24.27	1.	-4.36	-4.63	-3.46	-2.37	-6.91	-8.64	-7.07	-6.21	-6.16	-5.43
24.16	2.	-3.06	-2.63	-0.64	-3.04	-8.70	-7.30	-4.44	-3.80	-4.18	-3.88
24.04	3.	-2.20	-1.88	-0.60	1.83	-2.91	-5.18	-4.29	-2.68	-2.88	-2.81
23.93	4.	-1.38	-0.82	1.12	1.89	-5.62	-6.06	-2.69	-1.41	-1.74	-1.71
23.70	6.	-0.68	-0.49	0.48	4.29	1.58	-1.75	-2.52	-0.92	-1.03	-0.80
23.47	8.	-0.62	-0.33	1.20	4.51	-1.30	-4.30	-2.05	-0.59	-0.67	-0.75
23.25	10.	-0.96	-0.67	0.17	3.37	1.96	-1.08	-2.23	-0.87	-0.74	-0.61
22.68	15.	-0.97	-0.92	0.36	2.96	-1.95	-3.53	-2.12	-1.17	-0.98	-0.96
22.11	20.	-0.61	-0.76	-0.12	2.50	0.03	-1.48	-2.00	-1.19	-1.03	-0.79
20.98	30.	-0.71	-0.67	-0.48	0.48	-2.59	-3.76	-2.39	-1.75	-1.55	-1.30
		AXIAL VELOCITY - M/SEC									
24.27	1.	151.66	156.02	157.77	130.81	120.02	135.81	136.04	135.93	140.71	148.63
24.16	2.	158.04	160.61	162.40	134.70	127.17	148.65	150.77	147.79	149.91	155.45
24.04	3.	163.24	164.34	167.60	149.23	125.86	153.69	161.21	158.45	157.78	161.85
23.93	4.	167.93	168.59	169.96	150.82	128.71	158.97	169.34	165.79	165.49	167.34
23.70	6.	175.14	175.13	175.44	164.50	134.70	154.30	178.86	177.74	175.82	175.79
23.47	8.	180.47	180.02	178.90	164.96	140.92	163.65	184.36	183.99	182.14	181.70
23.25	10.	183.77	184.23	183.51	173.01	147.21	163.17	187.45	189.78	187.41	186.80
22.68	15.	193.95	195.05	194.06	180.78	166.18	184.28	197.13	198.74	197.67	197.63
22.11	20.	199.90	199.68	199.32	188.96	178.46	188.76	199.66	200.44	200.98	201.27
20.98	30.	205.35	205.48	205.16	190.28	187.52	194.85	200.97	200.65	201.65	201.40

TABLE VII. – Continued.

(b) Mass flow, 34.23 kg/sec

RADIUS CM	PERCENT PASSAGE HEIGHT	PERCENT GAP 0.	10.	20.	30.	40.	50.	60.	70.	80.	90.
		TOTAL PRESSURE - N/CM**2									
24.27	1.	16.17	16.26	16.27	15.45	15.34	15.78	15.86	15.84	15.83	16.02
24.16	2.	16.33	16.38	16.41	15.51	15.49	16.08	16.21	16.12	16.08	16.21
24.04	3.	16.47	16.50	16.52	15.89	15.29	16.09	16.47	16.38	16.27	16.37
23.93	4.	16.61	16.62	16.60	15.90	15.25	16.17	16.65	16.55	16.49	16.53
23.70	6.	16.77	16.74	16.75	16.33	15.29	15.92	16.81	16.80	16.75	16.77
23.47	8.	16.87	16.87	16.80	16.26	15.39	16.08	16.89	16.92	16.90	16.87
23.25	10.	16.96	16.93	16.87	16.40	15.52	15.95	16.90	17.05	16.99	17.01
22.68	15.	17.12	17.11	17.03	16.55	15.87	16.48	17.06	17.12	17.12	17.14
22.11	20.	17.19	17.19	17.15	16.79	16.24	16.70	17.10	17.09	17.10	17.12
20.98	30.	17.13	17.15	17.18	16.59	16.40	16.83	17.11	17.05	17.05	16.99
		TOTAL TEMPERATURE - DEG. K									
24.27	1.	353.01	356.29	355.57	355.74	355.34	352.87	352.80	354.40	353.46	354.82
24.16	2.	353.15	354.21	354.40	354.26	352.40	351.76	351.73	352.64	352.48	353.12
24.04	3.	353.71	352.96	353.95	353.53	349.87	351.54	351.53	351.76	352.03	352.06
23.93	4.	352.96	352.16	353.01	353.57	350.35	349.41	350.55	351.20	351.87	351.66
23.70	6.	351.26	351.81	351.93	352.71	348.78	347.75	348.07	349.20	349.95	350.94
23.47	8.	349.32	350.00	350.46	351.50	348.17	345.90	346.23	346.77	348.01	348.70
23.25	10.	347.29	348.46	349.25	350.32	347.07	344.44	344.93	345.36	346.41	347.05
22.68	15.	344.13	344.75	345.82	346.69	344.06	342.94	342.53	342.52	343.02	344.04
22.11	20.	341.80	341.99	342.90	343.60	341.90	341.08	340.56	340.42	340.78	341.14
20.98	30.	339.09	339.47	339.89	339.72	339.45	339.28	338.93	338.67	338.48	338.37
		ABSOLUTE FLOW ANGLE - DEG.									
24.27	1.	-4.05	-4.45	-2.90	-2.84	-8.61	-10.25	-8.03	-5.73	-5.55	-5.04
24.16	2.	-1.79	-2.04	0.05	-4.55	-11.50	-9.05	-5.26	-3.37	-3.28	-3.01
24.04	3.	-0.83	-0.54	1.01	2.41	-3.78	-6.83	-5.14	-2.59	-1.90	-1.86
23.93	4.	-0.42	0.51	2.77	1.65	-7.55	-8.15	-3.69	-1.43	-1.17	-1.04
23.70	6.	0.36	0.72	2.13	6.57	2.50	-3.33	-3.36	-1.18	-0.33	-0.26
23.47	8.	0.04	0.68	2.91	6.64	-1.54	-5.95	-2.84	-0.93	-0.48	-0.16
23.25	10.	-0.48	-0.08	1.09	5.13	3.23	-1.42	-2.47	-1.01	-0.54	-0.25
22.68	15.	-0.96	-0.29	1.06	4.34	-1.20	-3.91	-2.40	-1.26	-1.01	-0.76
22.11	20.	-0.75	-0.38	0.20	2.93	0.21	-1.60	-1.94	-1.12	-1.03	-1.10
20.98	30.	-0.45	-0.47	-0.04	1.17	-3.34	-4.32	-2.01	-1.16	-1.04	-1.13
		AXIAL VELOCITY - M/SEC									
24.27	1.	157.80	161.88	162.56	127.06	120.24	140.10	144.52	144.58	144.11	152.05
24.16	2.	164.71	166.84	168.07	130.38	126.74	153.42	159.32	156.46	155.26	160.09
24.04	3.	170.63	171.50	172.50	148.35	119.32	155.16	169.43	166.82	163.14	166.70
23.93	4.	175.68	175.98	175.24	149.76	117.47	157.72	176.21	173.42	171.29	172.79
23.70	6.	181.79	180.97	181.13	166.36	121.88	150.32	181.84	181.94	180.74	181.48
23.47	8.	185.46	185.39	183.19	164.60	128.90	157.14	184.87	186.13	186.02	185.29
23.25	10.	188.72	188.15	186.51	170.76	135.85	153.71	185.89	190.61	189.15	190.00
22.68	15.	194.82	194.81	192.93	178.24	154.02	174.93	192.74	194.56	194.51	195.44
22.11	20.	198.80	198.87	198.11	187.71	169.95	184.48	195.87	195.69	196.01	196.74
20.98	30.	201.41	202.12	203.06	186.41	180.27	192.61	200.64	199.02	198.97	197.50

TABLE VII. – Concluded.

(c) Mass flow, 34.01 kg/sec

RADIUS CM	PERCENT PASSAGE HEIGHT	PERCENT GAP 0.	10.	20.	30.	40.	50.	60.	70.	80.	90.
		TOTAL PRESSURE - N/CM**2									
24.27	1.	16.39	16.52	16.51	15.63	15.53	15.99	16.11	16.03	16.03	16.21
24.16	2.	16.56	16.65	16.65	15.69	15.63	16.27	16.44	16.31	16.27	16.40
24.04	3.	16.72	16.75	16.80	16.08	15.41	16.25	16.70	16.62	16.49	16.57
23.93	4.	16.86	16.88	16.88	16.11	15.35	16.34	16.88	16.82	16.72	16.75
23.70	6.	17.05	17.02	17.00	16.60	15.42	15.98	17.02	17.06	17.00	16.99
23.47	8.	17.15	17.11	17.06	16.53	15.50	16.10	17.10	17.17	17.13	17.11
23.25	10.	17.22	17.19	17.13	16.66	15.68	16.01	17.08	17.25	17.22	17.19
22.68	15.	17.32	17.31	17.23	16.74	16.01	16.52	17.22	17.25	17.25	17.27
22.11	20.	17.33	17.35	17.33	16.96	16.35	16.71	17.22	17.23	17.22	17.22
20.98	30.	17.25	17.25	17.29	16.72	16.50	16.94	17.25	17.21	17.16	17.13
		TOTAL TEMPERATURE - DEG. K									
24.27	1.	353.30	355.06	353.98	354.69	353.60	352.95	353.59	351.87	352.66	354.90
24.16	2.	352.99	354.17	354.06	353.62	351.74	351.86	351.79	351.67	352.39	353.52
24.04	3.	352.67	353.93	354.65	352.61	350.06	351.30	350.44	351.75	352.45	352.62
23.93	4.	353.84	352.84	353.18	354.78	350.38	350.47	351.23	352.16	352.44	352.82
23.70	6.	351.65	352.19	353.05	353.45	349.29	348.05	348.81	349.89	350.81	351.35
23.47	8.	350.28	349.53	351.35	352.91	348.66	346.71	347.15	347.95	348.92	349.58
23.25	10.	348.51	346.66	350.03	351.38	347.58	345.60	345.79	346.35	347.26	347.55
22.68	15.	345.08	345.13	346.10	347.40	345.47	343.39	343.17	343.49	343.73	344.23
22.11	20.	342.89	343.18	343.99	345.12	343.30	341.82	341.75	341.71	341.78	342.41
20.98	30.	340.04	340.20	341.06	340.43	340.49	339.32	339.71	340.08	340.13	339.70
		ABSOLUTE FLOW ANGLE - DEG.									
24.27	1.	-3.79	-4.45	-2.84	-2.90	-8.93	-10.17	-7.95	-5.42	-5.18	-5.08
24.16	2.	-1.72	-1.81	0.39	-4.43	-11.64	-9.17	-5.16	-3.18	-3.19	-2.91
24.04	3.	-0.64	-0.47	1.00	2.67	-3.79	-6.71	-5.08	-2.29	-1.60	-1.65
23.93	4.	0.22	0.64	3.11	2.27	-7.38	-8.42	-3.61	-1.23	-0.83	-0.71
23.70	6.	0.95	1.50	2.49	7.16	3.24	-3.37	-3.49	-1.24	-0.07	0.20
23.47	8.	0.68	1.24	3.10	7.51	-0.86	-6.03	-2.72	-0.62	0.23	0.40
23.25	10.	0.17	0.44	1.73	5.87	4.01	-1.24	-2.29	-1.05	-0.11	0.08
22.68	15.	-0.79	-0.23	1.26	4.85	-0.45	-3.49	-2.02	-0.85	-0.59	-0.51
22.11	20.	-0.73	-0.18	0.50	3.53	0.79	-1.12	-1.90	-0.89	-0.79	-0.48
20.98	30.	-0.45	-0.46	0.12	2.08	-2.88	-4.22	-1.75	-0.97	-0.89	-0.68
		AXIAL VELOCITY - M/SEC									
24.27	1.	160.26	165.21	164.98	128.49	121.98	142.33	148.34	145.33	145.86	153.40
24.16	2.	167.36	170.53	170.58	131.79	125.89	154.35	161.90	157.51	156.23	161.36
24.04	3.	173.38	174.46	176.37	149.54	117.89	154.93	171.41	169.44	165.17	168.14
23.93	4.	178.73	178.95	179.03	151.94	114.80	158.16	178.44	177.04	173.65	174.75
23.70	6.	185.17	184.34	183.99	169.91	120.79	146.49	183.18	184.91	183.58	183.26
23.47	8.	188.83	187.47	186.37	168.50	126.39	151.82	186.44	188.87	188.03	187.53
23.25	10.	191.61	190.22	189.07	173.94	136.06	150.12	186.52	191.63	191.04	190.25
22.68	15.	195.94	195.56	193.67	178.73	153.43	170.90	192.56	193.39	193.47	194.24
22.11	20.	198.01	198.73	198.34	187.83	168.21	179.70	194.70	194.98	194.58	194.78
20.98	30.	199.88	200.13	201.39	185.12	178.03	190.82	199.70	198.86	197.44	196.50

TABLE VIII. – CIRCUMFERENTIAL DISTRIBUTIONS AT SECOND-STAGE STATOR EXIT

(a) Mass flow, 34.63 kg/sec

RADIUS CM	PERCENT PASSAGE HEIGHT	PERCENT GAP 0.	10.	20.	30.	40.	50.	60.	70.	80.	90.
		TOTAL PRESSURE - N/CM**2									
23.54	1.	22.15	22.35	22.48	22.57	22.63	22.04	21.32	21.60	21.57	21.60
23.45	2.	22.29	22.51	22.66	22.76	22.79	22.20	21.42	21.90	21.98	21.88
23.37	3.	22.39	22.61	22.81	22.89	22.92	22.49	21.54	21.96	22.31	22.13
23.29	4.	22.48	22.70	22.90	22.97	22.99	22.64	21.50	22.09	22.52	22.39
23.12	6.	22.66	22.87	23.02	23.10	23.11	22.89	21.79	21.95	22.81	22.80
22.95	8.	22.88	23.05	23.21	23.30	23.24	22.98	21.76	22.08	23.01	23.04
22.78	10.	23.07	23.17	23.30	23.36	23.37	23.15	22.13	22.01	23.03	23.16
22.36	15.	23.46	23.52	23.56	23.56	23.52	23.41	22.37	22.14	23.13	23.37
21.95	20.	23.64	23.67	23.68	23.64	23.59	23.52	22.80	22.36	22.98	23.50
21.11	30.	23.72	23.74	23.74	23.70	23.71	23.65	22.96	22.68	23.26	23.61
		TOTAL TEMPERATURE - DEG. K									
23.54	1.	392.96	394.30	393.58	394.36	392.52	398.87	393.73	392.83	394.26	395.16
23.45	2.	393.45	393.95	393.79	393.95	393.23	399.68	393.20	393.49	394.13	394.44
23.37	3.	394.41	393.91	394.67	393.91	394.52	407.19	392.67	395.05	398.20	393.60
23.29	4.	393.74	392.60	393.51	393.26	393.67	394.41	392.96	392.92	385.81	393.69
23.12	6.	393.46	394.07	393.38	393.13	393.27	394.47	392.57	393.12	394.26	394.55
22.95	8.	393.25	393.28	392.99	392.62	392.71	393.41	392.05	391.84	393.24	393.62
22.78	10.	392.72	392.34	392.04	391.73	391.68	392.71	391.99	390.83	391.49	392.19
22.36	15.	390.13	390.13	389.54	389.16	389.01	390.24	389.32	387.78	388.72	389.49
21.95	20.	387.22	387.27	386.85	386.11	386.30	387.32	386.82	385.16	385.98	386.66
21.11	30.	382.42	382.59	382.49	382.30	382.36	383.27	383.07	381.81	382.24	382.58
		ABSOLUTE FLOW ANGLE - DEG.									
23.54	1.	-7.24	-6.28	-5.05	-4.03	-2.02	0.76	-5.95	-7.50	-5.00	-5.08
23.45	2.	-5.36	-4.39	-3.24	-2.11	-0.17	2.62	-5.21	-6.58	-3.39	-3.03
23.37	3.	-3.88	-3.25	-2.01	-0.98	0.72	3.97	-1.41	-5.94	-2.45	-1.18
23.29	4.	-2.97	-3.27	-1.41	-0.47	1.25	5.40	-0.36	-5.25	-1.39	-0.03
23.12	6.	-1.24	-1.14	-0.40	0.43	1.81	5.80	4.54	-3.80	-1.24	1.28
22.95	8.	-0.08	-0.05	0.42	1.16	2.32	6.28	5.15	-3.84	-0.84	1.58
22.78	10.	0.98	0.94	1.22	1.78	2.62	5.56	6.86	-2.56	-1.36	1.46
22.36	15.	1.87	2.02	2.29	2.46	2.82	5.48	6.62	-2.45	-1.88	0.44
21.95	20.	1.59	1.79	2.06	2.16	2.34	4.37	5.27	-0.50	-2.62	-0.58
21.11	30.	0.21	0.42	0.69	0.83	1.15	3.11	2.86	-0.40	-2.75	-1.16
		AXIAL VELOCITY - M/SEC									
23.54	1.	146.64	153.59	158.02	160.93	162.66	145.27	115.14	126.75	126.06	127.42
23.45	2.	152.00	159.20	163.91	167.17	167.78	150.98	120.21	138.58	142.07	138.65
23.37	3.	155.91	162.62	168.88	171.13	171.91	161.73	125.68	141.48	154.46	147.96
23.29	4.	159.00	165.48	171.47	173.34	173.81	163.40	124.54	145.99	158.93	156.62
23.12	6.	165.07	171.25	175.28	177.24	177.59	170.91	135.96	141.93	169.58	169.22
22.95	8.	171.80	176.54	180.45	182.66	181.22	173.48	135.23	146.95	175.29	176.14
22.78	10.	177.25	179.95	183.16	184.57	184.64	178.62	148.56	144.94	175.95	179.49
22.36	15.	187.51	189.14	189.87	189.76	188.76	185.67	156.88	150.31	179.00	185.41
21.95	20.	192.22	192.92	193.14	191.89	190.85	189.09	170.43	157.91	175.48	188.93
21.11	30.	195.07	195.62	195.42	194.51	194.68	193.45	176.67	169.09	183.94	192.48

TABLE VIII. – Continued.

(b) Mass flow, 34.23 kg/sec

RADIUS CM	PERCENT PASSAGE HEIGHT	PERCENT GAP 0.	10.	20.	30.	40.	50.	60.	70.	80.	90.
		TOTAL PRESSURE - N/CM**2									
23.54	1.	24.07	24.21	24.45	24.69	24.92	24.57	23.36	23.98	24.28	24.29
23.45	2.	24.29	24.35	24.51	24.78	25.04	24.71	23.45	24.12	24.67	24.71
23.37	3.	24.55	24.51	24.57	24.74	25.01	25.00	23.57	23.92	24.89	25.01
23.29	4.	24.81	24.67	24.66	24.81	25.07	25.07	23.56	23.88	25.08	25.28
23.12	6.	25.20	25.08	24.92	24.92	25.14	25.20	24.09	23.48	25.04	25.53
22.95	8.	25.37	25.17	25.07	25.08	25.19	25.28	24.23	23.54	25.12	25.56
22.78	10.	25.41	25.30	25.24	25.23	25.28	25.40	24.65	23.56	24.90	25.56
22.36	15.	25.54	25.47	25.42	25.52	25.61	25.64	24.81	23.71	24.74	25.53
21.95	20.	25.44	25.64	25.65	25.67	25.73	25.73	25.08	24.32	24.66	25.45
21.11	30.	25.67	25.66	25.66	25.69	25.70	25.71	25.01	24.62	24.91	25.57
		TOTAL TEMPERATURE - DEG. K									
23.54	1.	404.63	407.13	406.30	408.06	409.39	407.62	406.38	408.64	407.06	407.32
23.45	2.	405.37	406.40	405.87	406.83	407.36	407.04	404.87	406.23	405.85	406.01
23.37	3.	406.60	405.62	405.25	405.82	404.94	407.54	403.09	404.46	404.89	405.14
23.29	4.	406.40	405.77	406.18	405.48	406.18	405.90	404.37	403.45	405.31	404.25
23.12	6.	405.67	406.22	405.43	405.04	404.96	405.59	403.24	401.66	403.38	404.55
22.95	8.	404.70	405.48	405.32	404.71	404.14	404.67	404.30	400.50	402.28	402.62
22.78	10.	403.26	404.81	404.70	404.36	403.59	403.83	404.04	399.52	401.10	401.47
22.36	15.	400.53	401.57	402.14	402.19	401.30	401.83	401.66	397.66	397.81	399.06
21.95	20.	396.94	397.67	398.56	398.55	397.75	398.62	398.25	395.42	394.69	395.77
21.11	30.	382.62	391.48	391.56	391.52	391.41	392.25	391.91	390.28	389.82	390.84
		ABSOLUTE FLOW ANGLE - DEG.									
23.54	1.	-3.28	-4.09	-5.29	-5.27	-3.31	1.90	-3.71	-8.57	-4.57	-1.76
23.45	2.	-0.84	-1.61	-2.66	-2.92	-1.38	3.91	-2.57	-7.51	-3.16	-0.36
23.37	3.	0.96	0.63	-0.37	-1.50	-0.35	4.55	1.85	-6.00	-3.10	0.68
23.29	4.	2.34	1.92	0.76	-0.44	0.56	5.84	3.64	-5.52	-2.33	1.25
23.12	6.	3.73	3.98	3.64	2.42	2.04	5.74	8.31	-1.66	-2.83	1.60
22.95	8.	3.96	4.39	4.15	3.33	2.95	6.22	8.65	-2.02	-2.48	1.35
22.78	10.	3.74	4.28	4.56	4.11	3.58	5.69	10.12	1.69	-3.06	1.06
22.36	15.	2.88	3.23	3.51	3.75	3.97	5.95	10.06	2.32	-2.81	-0.23
21.95	20.	1.88	2.07	2.40	2.73	3.16	4.96	7.41	2.66	-1.45	-0.88
21.11	30.	1.32	1.35	1.36	1.47	1.80	3.51	5.58	1.71	-1.17	-0.95
		AXIAL VELOCITY - M/SEC									
23.54	1.	140.10	145.14	152.29	159.53	166.76	156.51	113.70	136.37	147.21	148.14
23.45	2.	147.90	150.18	154.58	162.60	169.89	160.56	117.83	141.46	159.16	160.72
23.37	3.	156.49	155.20	156.92	161.76	169.09	168.70	122.86	135.27	165.58	169.12
23.29	4.	163.97	160.06	159.78	163.92	171.00	170.06	122.64	133.95	171.08	176.00
23.12	6.	174.56	171.51	167.00	167.11	172.92	173.84	140.90	119.84	170.13	182.64
22.95	8.	178.94	174.10	171.59	171.82	174.48	176.07	145.92	123.06	172.41	183.41
22.78	10.	180.07	177.70	176.11	175.76	177.02	179.51	158.30	124.23	166.84	183.64
22.36	15.	183.86	182.43	181.24	183.72	185.59	185.68	163.50	131.21	163.21	183.58
21.95	20.	182.03	186.74	187.25	187.54	188.82	188.61	172.28	152.27	161.76	182.19
21.11	30.	186.14	188.12	188.14	188.79	188.90	189.17	172.28	162.43	169.93	185.95

TABLE VIII. – Concluded.

(c) Mass flow, 34.01 kg/sec

RADIUS CM	PERCENT PASSAGE HEIGHT	PERCENT GAP 0.	10.	20.	30.	40.	50.	60.	70.	80.	90.
		TOTAL PRESSURE - N/CM**2									
23.54	1.	24.26	24.39	24.65	24.93	25.22	24.78	23.62	24.24	24.50	24.47
23.45	2.	24.49	24.53	24.72	25.04	25.28	24.90	23.71	24.39	24.87	24.87
23.37	3.	24.65	24.68	24.74	24.92	25.27	25.15	23.76	24.10	25.06	25.20
25.32	4.	24.96	24.78	24.82	25.02	25.33	25.27	23.78	24.07	25.30	25.44
23.12	6.	25.29	25.17	25.06	25.06	25.35	25.43	24.33	23.70	25.24	25.68
22.95	8.	25.46	25.31	25.18	25.20	25.47	25.51	24.39	23.77	25.38	25.72
22.78	10.	25.49	25.42	25.33	25.34	25.52	25.59	24.81	23.69	25.11	25.77
22.36	15.	25.72	25.68	25.65	25.71	25.77	25.84	24.98	23.90	24.91	25.68
21.95	20.	25.76	25.76	25.77	25.78	25.86	25.86	25.14	24.49	24.84	25.62
21.11	30.	25.80	25.78	25.74	25.78	25.79	25.82	25.12	24.77	25.01	25.66
		TOTAL TEMPERATURE - DEG. K									
23.54	1.	402.44	405.79	405.10	406.52	406.65	405.64	405.82	405.03	405.97	407.08
23.45	2.	403.84	405.66	405.22	405.66	405.86	405.91	404.34	404.48	405.35	406.08
23.37	3.	404.67	405.71	405.37	403.86	404.99	406.88	401.90	404.08	404.75	405.22
25.32	4.	404.94	405.71	405.59	404.56	404.96	405.23	403.12	401.97	403.80	404.04
23.12	6.	404.93	404.86	405.20	405.00	404.08	404.69	404.25	400.80	402.71	403.21
22.95	8.	405.06	404.89	405.27	405.16	404.12	404.71	404.37	400.79	402.73	403.18
22.78	10.	403.64	404.22	404.53	404.11	403.18	404.30	404.22	400.12	401.78	402.10
22.36	15.	401.01	401.49	402.08	402.00	401.60	401.42	401.31	397.69	398.20	399.01
21.95	20.	397.59	398.28	398.92	398.57	398.13	398.09	398.34	395.80	395.13	396.48
21.11	30.	391.55	391.89	392.37	391.67	391.38	391.69	391.90	390.94	390.99	391.68
		ABSOLUTE FLOW ANGLE - DEG.									
23.54	1.	-3.72	-4.62	-5.36	-5.44	-3.40	1.74	-4.09	-8.69	-4.53	-1.78
23.45	2.	-1.27	-2.41	-3.05	-3.13	-1.41	3.72	-2.72	-7.50	-3.12	-0.36
23.37	3.	0.86	-0.05	-0.84	-1.64	-0.45	4.57	1.53	-6.05	-2.90	0.70
25.32	4.	1.97	1.46	0.07	-0.80	0.41	5.78	3.41	-5.32	-2.25	1.27
23.12	6.	3.48	3.75	2.81	1.72	1.69	5.63	8.34	-1.76	-2.65	1.59
22.95	8.	3.79	4.17	3.85	3.07	2.81	6.19	8.58	-2.14	-2.46	1.38
22.78	10.	3.67	4.09	4.21	3.70	3.39	5.63	9.99	1.54	-2.83	1.00
22.36	15.	2.88	3.20	3.50	3.73	3.94	6.05	9.96	2.05	-2.80	-0.22
21.95	20.	1.89	2.07	2.36	2.70	3.11	4.91	7.17	2.30	-1.63	-0.94
21.11	30.	1.37	1.47	1.46	1.53	1.73	3.45	5.48	1.59	-1.41	-1.01
		AXIAL VELOCITY - M/SEC									
23.54	1.	140.45	145.04	152.67	161.21	169.47	157.16	117.65	138.83	148.66	148.31
23.45	2.	148.81	150.22	155.72	164.76	171.43	160.73	121.68	144.39	159.87	160.25
23.37	3.	154.14	155.03	156.94	161.55	171.20	168.08	123.60	135.64	165.53	169.46
25.32	4.	163.10	158.39	159.50	164.77	173.05	170.87	124.61	134.79	171.90	175.68
23.12	6.	172.35	169.14	166.36	166.64	173.95	175.40	143.54	122.32	170.84	181.75
22.95	8.	177.27	173.36	170.01	170.71	177.42	177.66	146.06	125.73	174.92	183.39
22.78	10.	178.29	176.47	174.24	174.64	178.80	180.14	158.50	123.61	168.26	184.95
22.36	15.	184.63	183.63	183.00	184.35	185.78	186.52	163.96	132.96	163.80	183.52
21.95	20.	186.19	186.33	186.79	186.83	188.36	187.94	170.16	153.03	162.99	182.69
21.11	30.	188.30	188.04	187.15	187.98	188.06	188.55	171.84	163.16	169.51	185.31

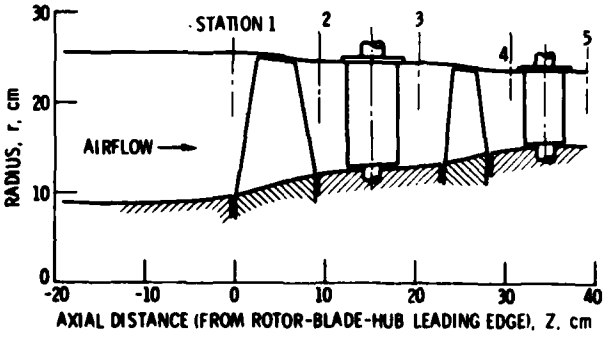

Figure 1. - Flow path of two-stage low-aspect-ratio fan.

Flow path coordinates

Axial distance, Z, cm	Radius, r, cm	
	Outer	Inner
-13.093	25.654	8.994
-8.016	25.654	8.903
-2.936	25.654	9.093
[a]-.203	25.651	9.543
2.144	25.570	10.160
4.684	25.128	10.973
7.224	24.681	11.565
[a]9.764	24.460	11.902
12.304	24.384	12.139
14.844	↓	12.438
17.384	↓	12.822
19.924	↓	13.025
[a]20.803	↓	13.038
22.464	24.328	13.152
25.004	23.993	13.627
27.544	23.655	14.371
[a]30.084	23.622	14.699
32.177	↓	14.849
36.754	↓	15.237
[a]38.850	↓	15.240
42.784	↓	15.240

[a]Instrument survey plane.

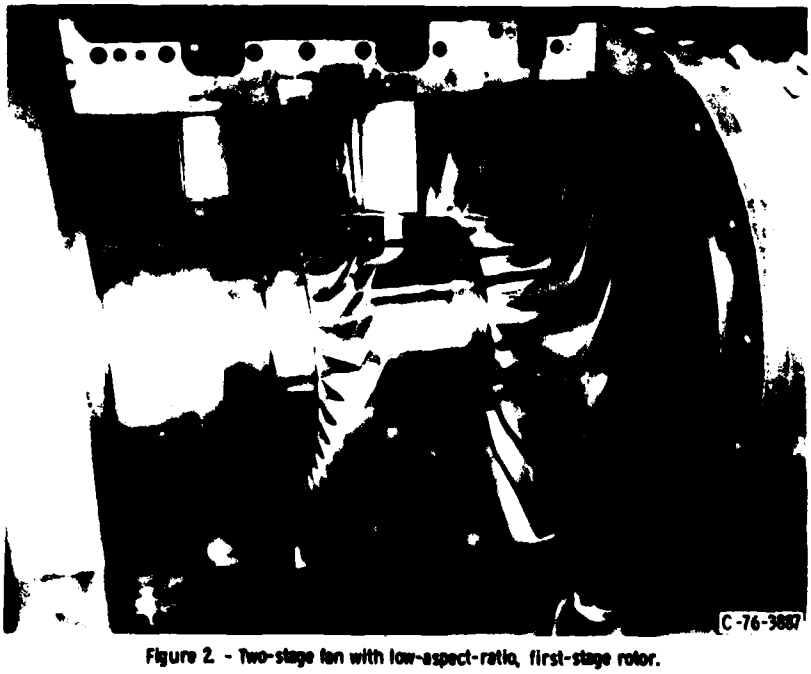

Figure 2. - Two-stage fan with low-aspect-ratio, first-stage rotor.

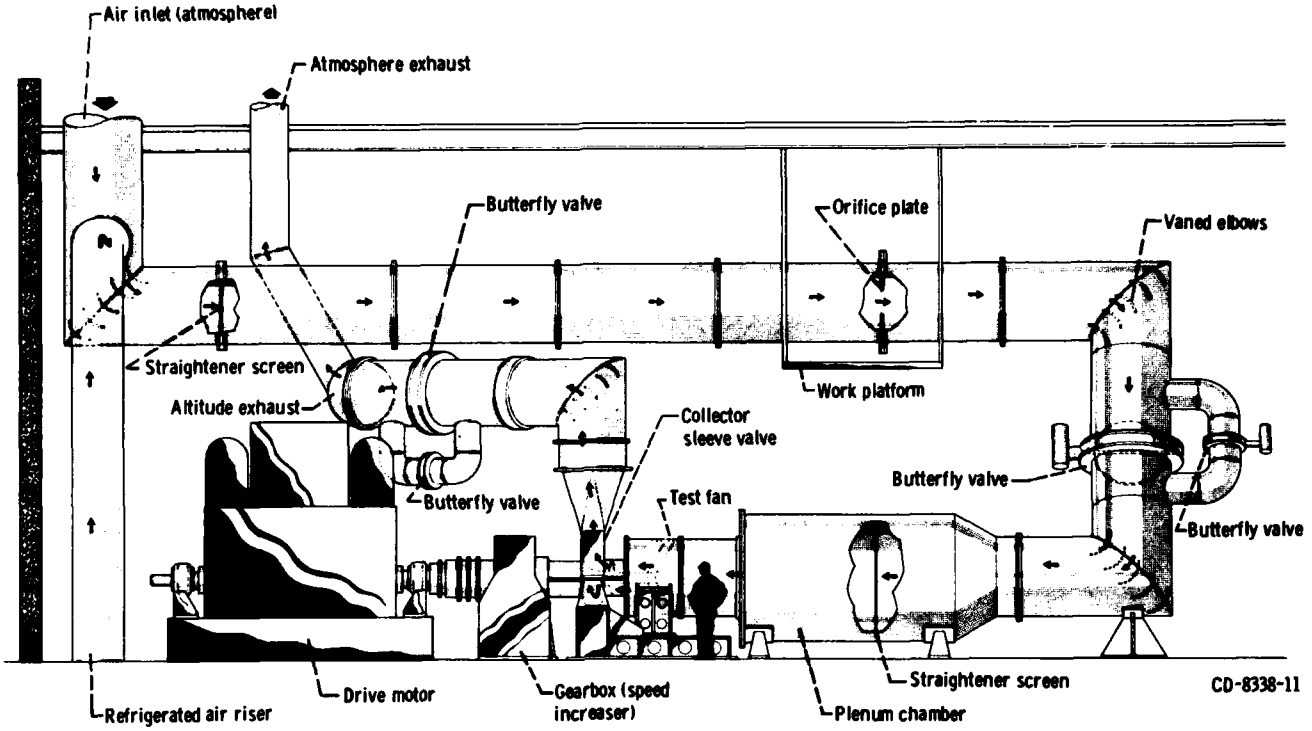

Figure 3. - Multistage compressor test facility.

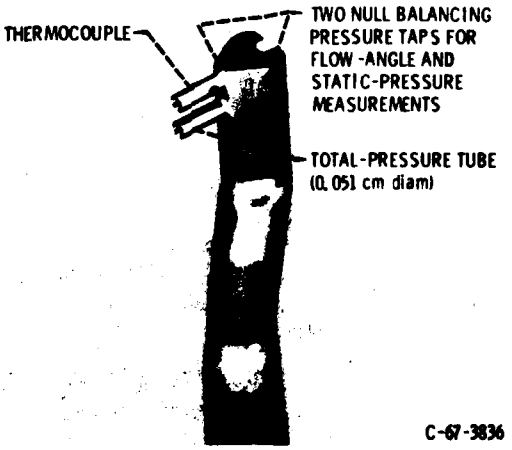

Figure 4. - Combination total-pressure, static-pressure, total-temperature, and flow-angle probe (double barrel).

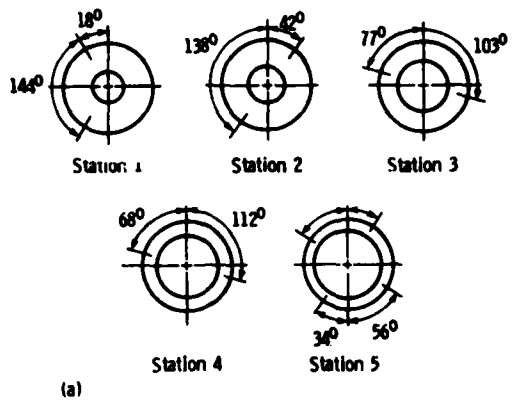

(a) Combination probes.
(b) Static pressure taps.

Figure 5. - Circumferential locations of instrumentation at measuring stations (looking downstream).

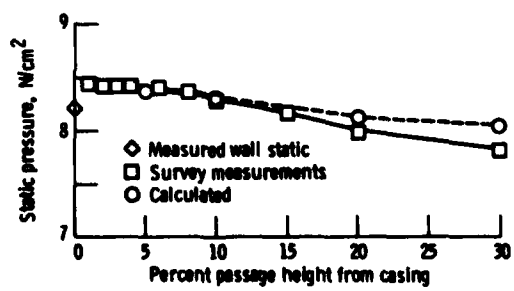

Figure 6. - Comparison of measured and calculated static pressure at station one.

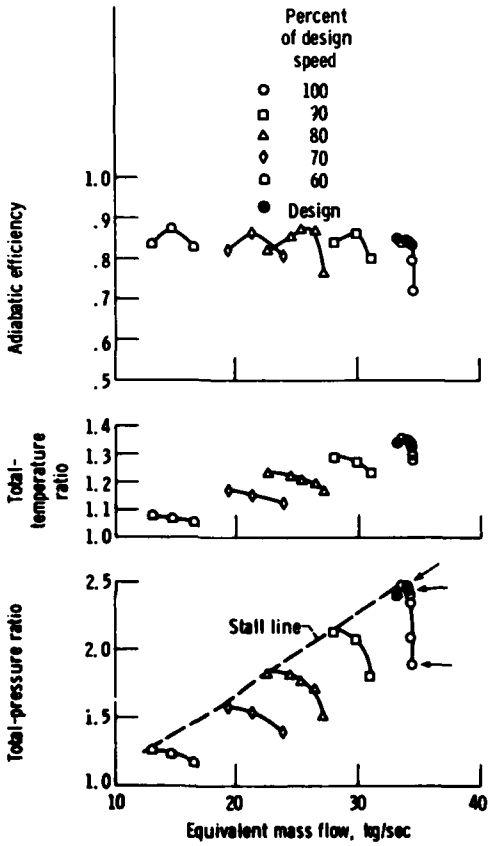

Figure 7. - Overall performance of two-stage, low-aspect-ratio fan.

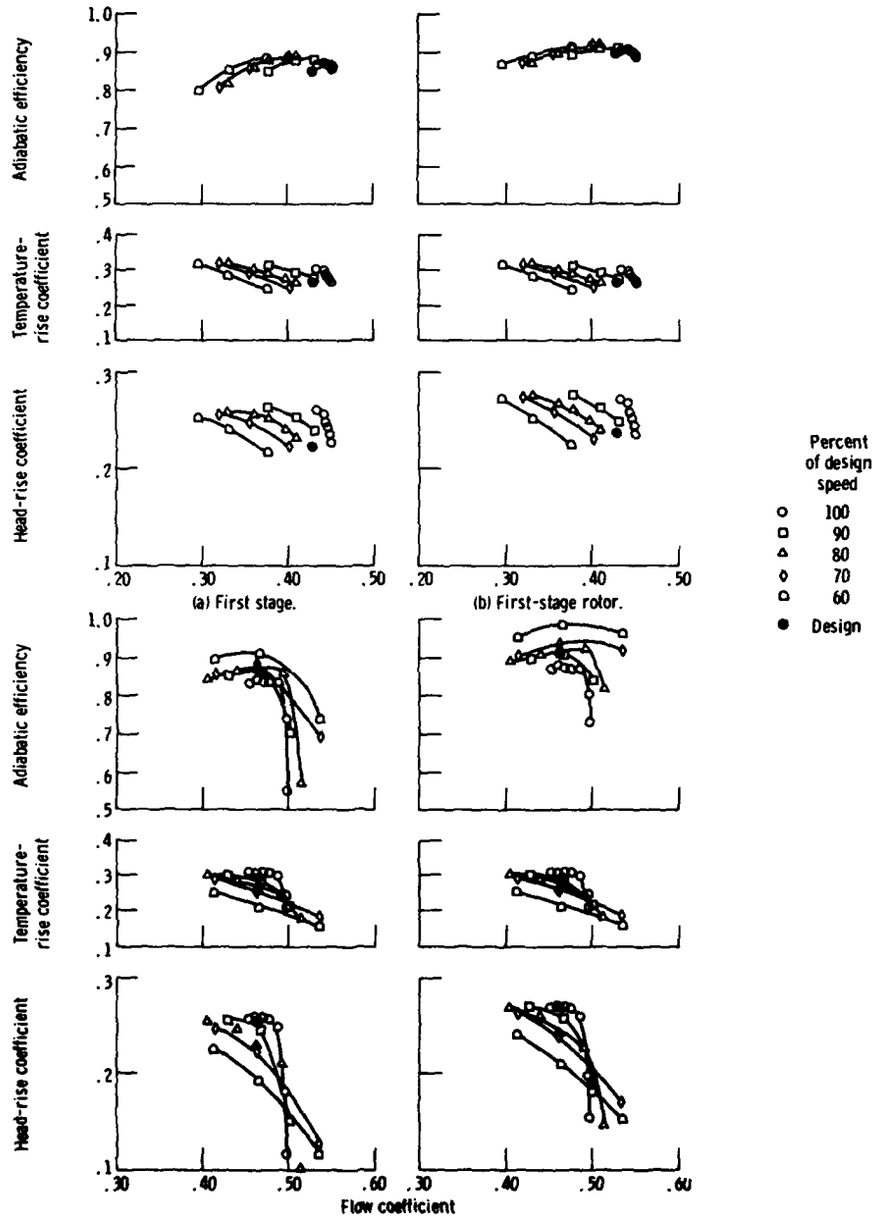

Figure 8. - Dimensionless overall performance.

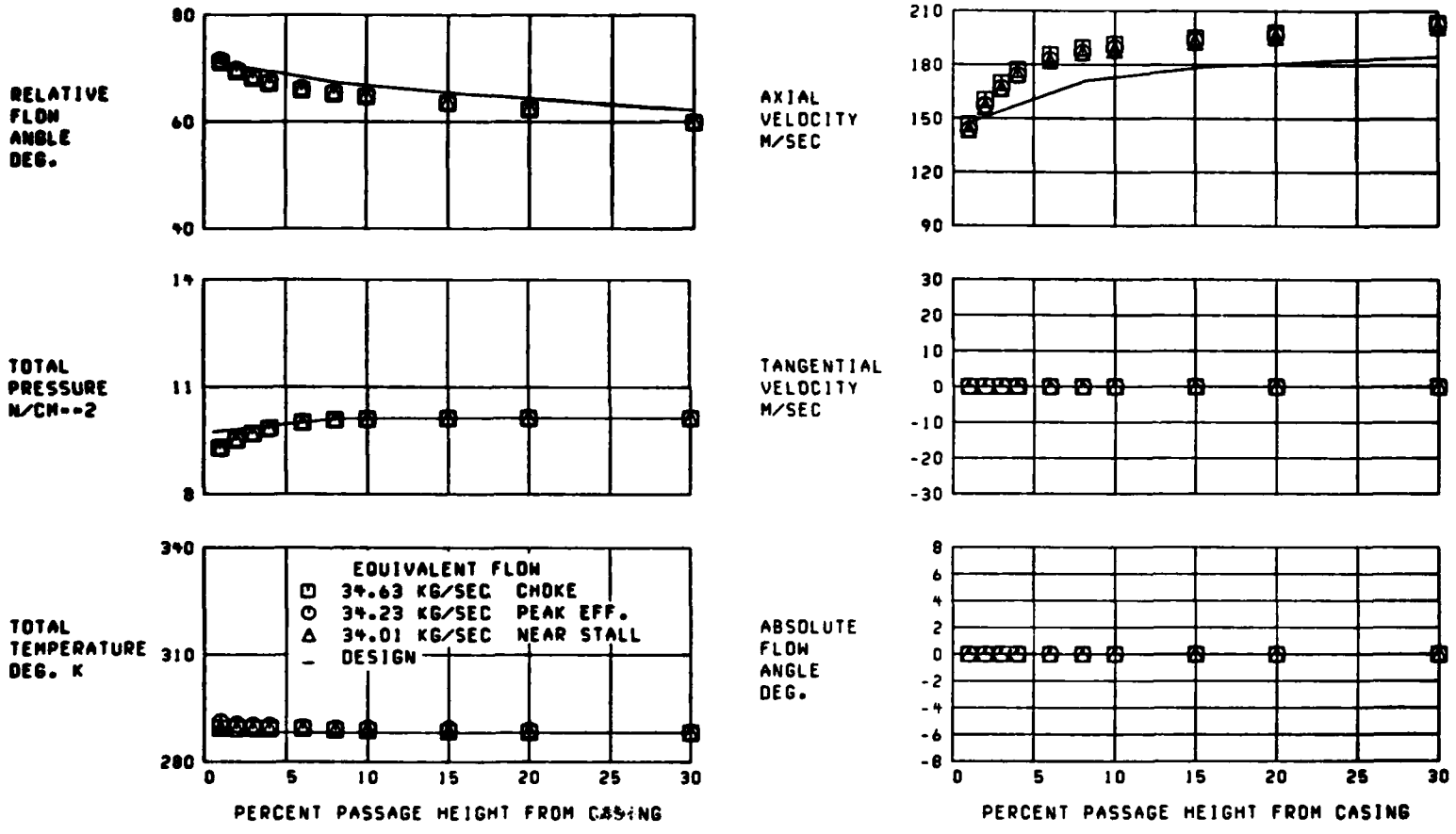

Figure 9. Radial distributions at measuring station 1, first-stage rotor inlet.

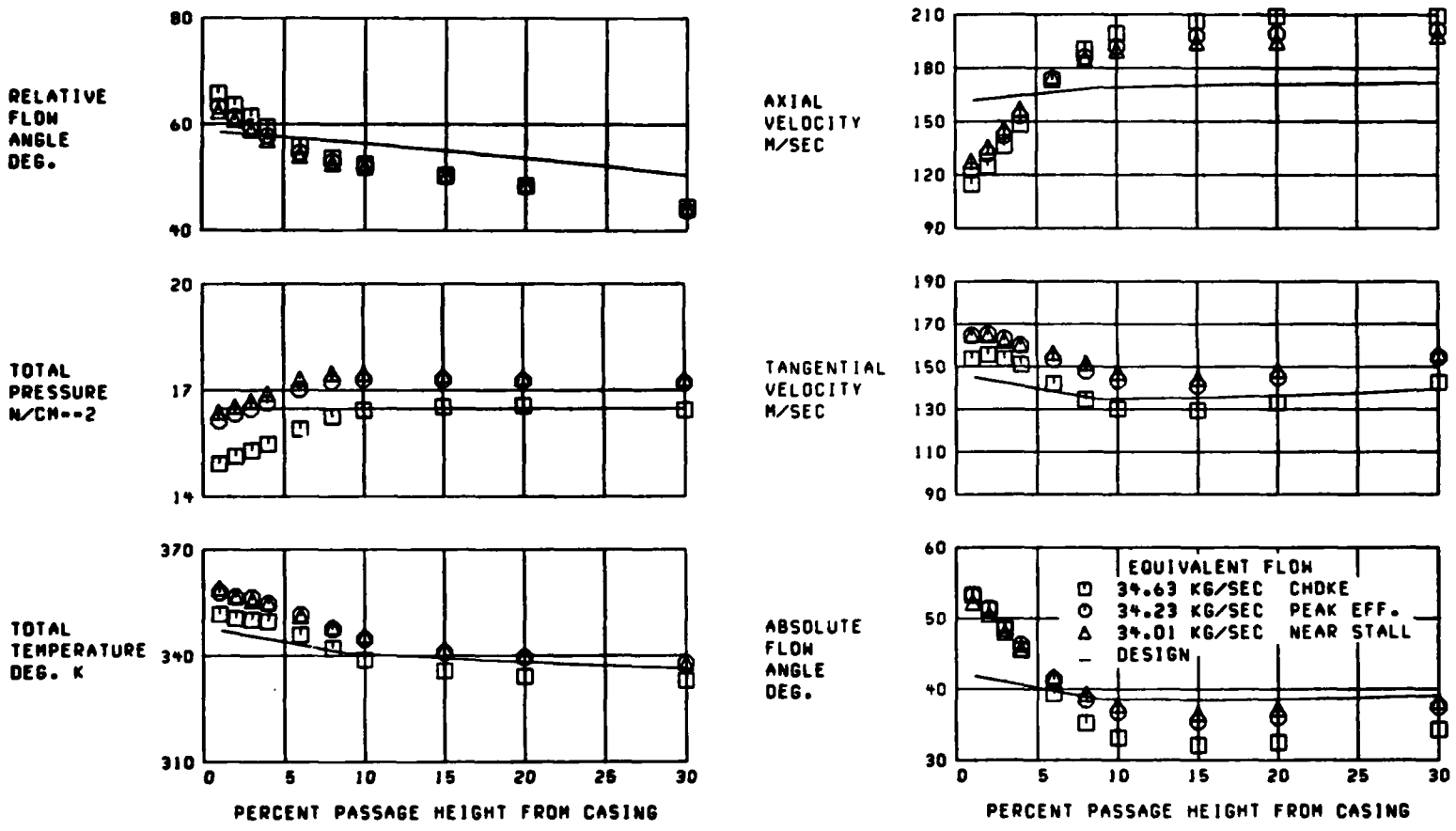

Figure 10. - Radial distributions at measuring station 2, first-stage rotor exit.

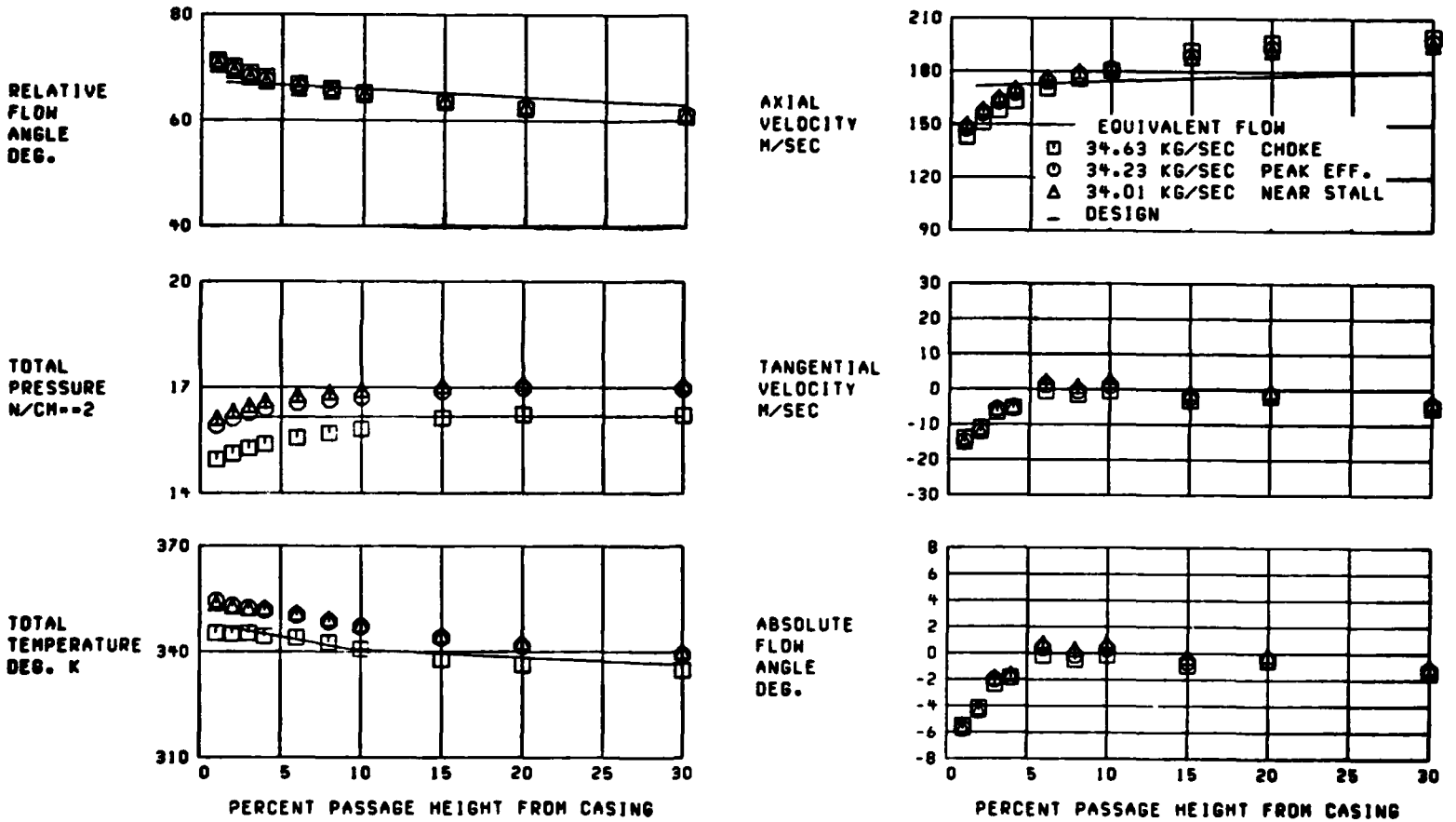

Figure 11. - Radial distributions at measuring station 3, first-stage stator exit.

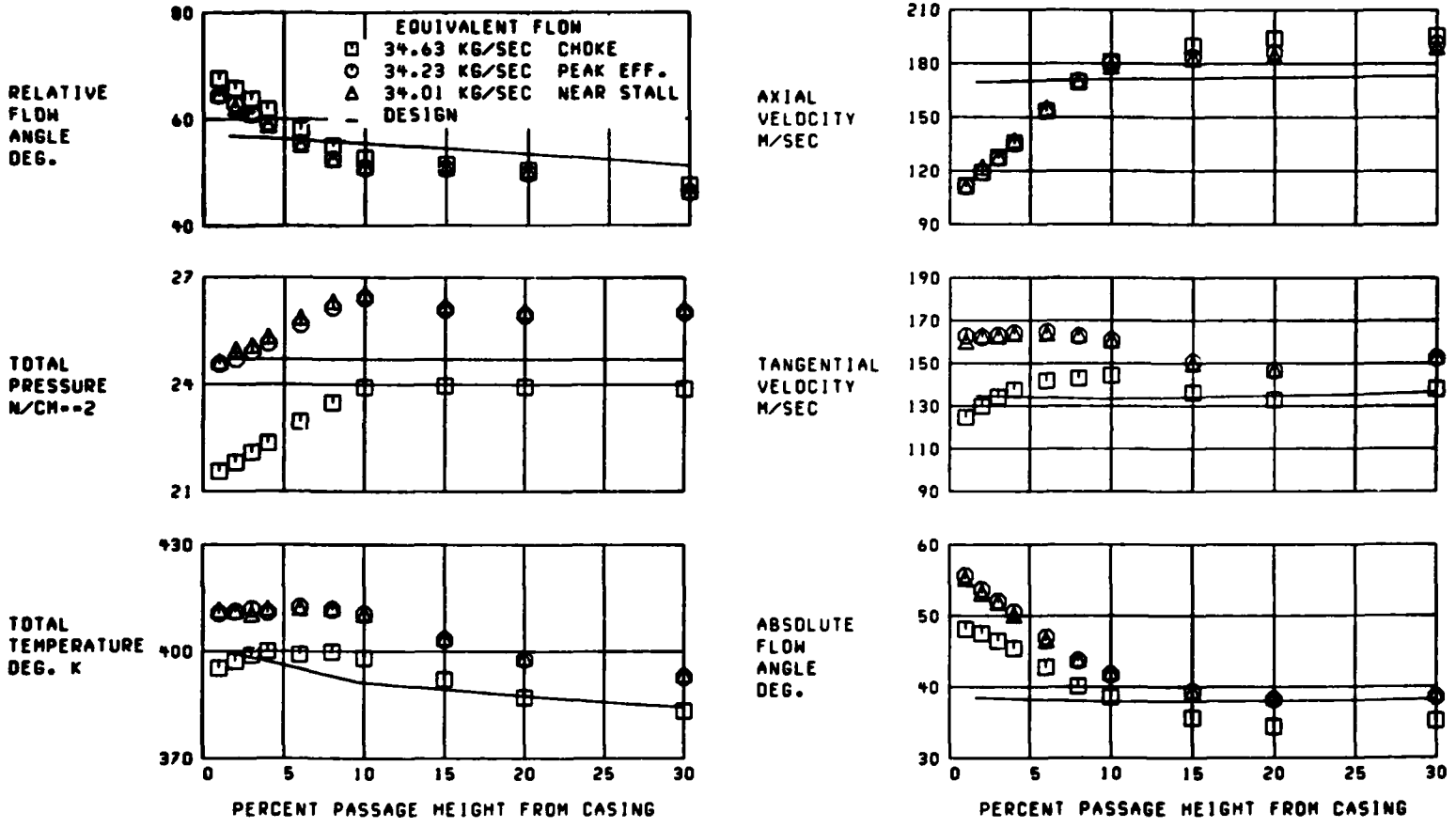

Figure 12. - Radial distributions at measuring station 4, second-stage rotor exit.

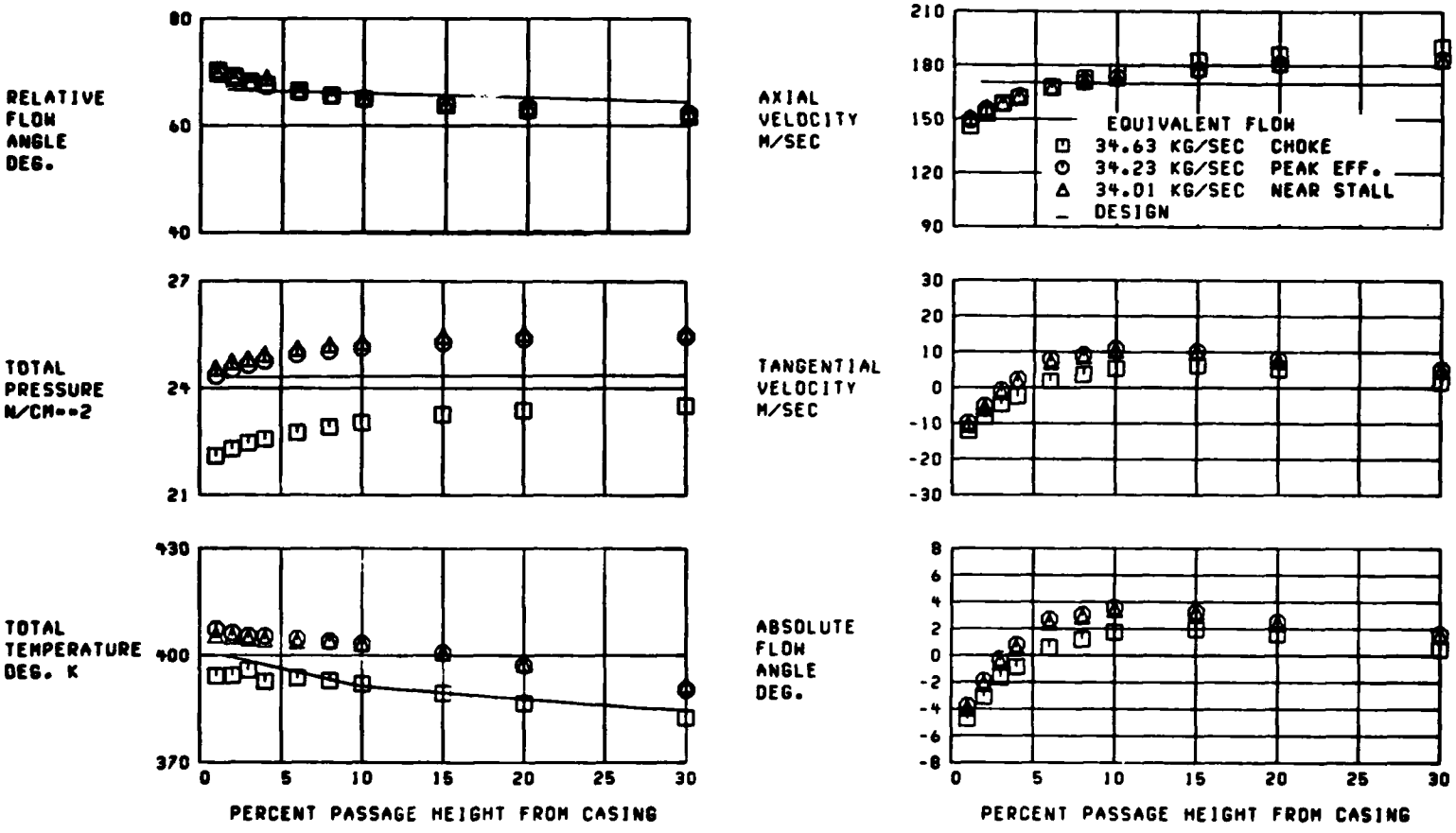

Figure 13. - Radial distributions at measuring station 5, second-stage stator exit.

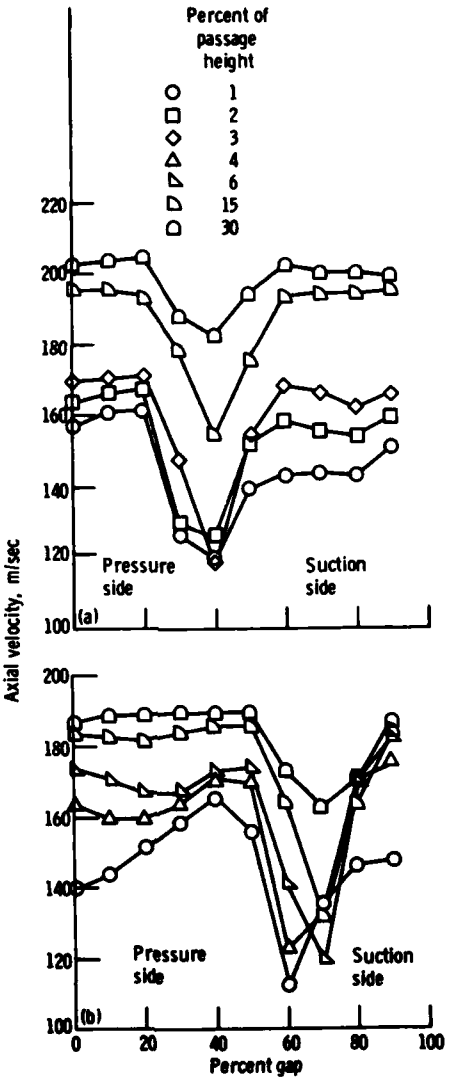

(a) First-stage stator exit.

(b) Second-stage stator exit.

Figure 14. - Circumferential variation of axial velocity at stator exits. Mass flow, 34.23 kg/sec.

1. Report No.	2. Government Accession No.	3. Recipient's Catalog No.
Corrected Copy NASA TP-2052 AVRADCOM TR 81-C-28	AD-A138370	

4. Title and Subtitle

Detailed Flow Measurements in Casing Boundary Layer of 429-Meter-Per-Second-Tip-Speed Two-Stage Fan

5. Report Date

January 1984

6. Performing Organization Code

505-32-22

7. Author(s)

William T. Gorrell

8. Performing Organization Report No.

E-219

10. Work Unit No.

9. Performing Organization Name and Address

Propulsion Laboratory
AVRADCOM Research and Technology Laboratories
Lewis Research Center
Cleveland, Ohio 44135

11. Contract or Grant No.

13. Type of Report and Period Covered

Technical Paper

12. Sponsoring Agency Name and Address

National Aeronautics and Space Administration
Washington, D.C. 20546 and
U.S. Army Aviation Research and Development Command
St. Louis, Missouri 63166

14. Sponsoring Agency Code

15. Supplementary Notes

16. Abstract

Detailed flow measurements between all blade rows were taken in the outer 30 percent of passage height of a two-stage fan. Tabulations of the detailed flow measurements are included. Results of these measurements revealed the steep axial velocity profiles near the casing. The axial velocity profile near the casing at the rotor exits was much steeper than at the stator exits. The data also show overturning of the flow at the tip at the stator exits. The effect of mixing is shown by the redistribution of the first-stage rotor-exit total temperature profile as it passes through the following stator.

17. Key Words (Suggested by Author(s))	18. Distribution Statement
Turbomachinery	Unclassified - unlimited STAR Category 07

19. Security Classif. (of this report)	20. Security Classif. (of this page)	21. No. of pages	22. Price*
Unclassified	Unclassified	32	A03

*For sale by the National Technical Information Service, Springfield, Virginia 22161

NASA-Langley, 1984

END

DATE
FILMED

4-84

DTIC